Hydrogeochemistry and gas compositions of the Uinta Basin: A regional-scale overview

Ye Zhang, Carl W. Gable, George A. Zyvoloski, and Lynn M. Walter

ABSTRACT

The geochemistry of formation fluids (water and hydrocarbon gases) in the Uinta Basin, Utah, is evaluated at the regional scale based on fluid sampling and compilation of past records. The deep formation water is dominated by Na-Cl type where halite dissolution has the greatest effects on water chemistry. Its distribution and composition is controlled by both the lithology of geological formations and regional hydrodynamics. The origin of the saline waters in the southeastern basin is interpreted to be a mix of ancient evaporatively concentrated seawater with meteoric water recharged in the geological past, which has experienced water-rock interactions. At the basin scale, three-dimensional mapping of the dissolved solid contents further reveals that (1) in the northern Uinta Basin bordering the Uinta Mountains, significant flushing of the deep basinal brines up to 6-km (3.7-mi) depth by meteoric water has occurred, and (2) in the central basin groundwater discharge areas along the Green River Valley, regional upwelling of saline waters from 2- to 3-km (1.2- to 1.8-mi) depth is occurring. Moreover, gas composition and water-gas stable isotope characteristics in the central to southeastern basin indicate the presence of a deep, thermogenic, and regionally continuous gas deposit. In particular, gases sampled in this region from the Wasatch Formation and Mesaverde Group indicate a similar source rock (type III kerogen of the deeply buried, thermally mature Mesaverde Group in the central to northern basin) as well as migration from the Natural Buttes gas field toward the southeastern basin. Evidence for biogenic methane formation is observed only in the upper Green River Formation in the

AUTHORS

YE ZHANG ~ *Department of Geology and Geophysics, University of Wyoming, 1000 University Avenue, Laramie, Wyoming 82071; yzhang9@uwyo.edu*

Ye Zhang received her B.S. degree in hydrogeology and engineering geology from Nanjing University, P.R. China (1998); her M.S. degree in hydrogeology from the University of Minnesota (2004); and her Ph.D. in hydrogeology from Indiana University (2005). She is currently an assistant professor of geology at the University of Wyoming. Her research interests include geological modeling and fluid-flow simulation, scientific computing, and aqueous and hydrocarbon gas geochemistry.

CARL W. GABLE ~ *Computational Earth Science Group, Earth and Environmental Sciences Division, Los Alamos National Laboratory, Los Alamos, New Mexico 87545; gable@lanl.gov*

Carl Gable received his A.B. degree in geophysics from the University of California, Berkeley, and his M.S. degree in applied physics and Ph.D. in geophysics from Harvard University. Since 1990 he has been a staff scientist at Los Alamos National Laboratory working in various areas of computational fluid dynamics and continuum mechanics applied to geologic systems. His main focus is in research and application of finite element mesh generation, computational geometry, and flow and transport in porous media.

GEORGE A. ZYVOLOSKI ~ *Computational Earth Science Group (EES-16), Los Alamos National Laboratory, Los Alamos, New Mexico 87545; gaz@lanl.gov*

George A. Zyvoloski received his B.S. (1971) and M.S. (1972) degrees and Ph.D. (1975) in mechanical engineering from the University of California, Santa Barbara. He has been at Los Alamos since 1979, where he has developed numerical methods and software to solve subsurface flow and transport problems related to geothermal energy extraction and radionuclide transport as well as conventional and unconventional oil and gas production.

LYNN M. WALTER ∼ *Department of Geological Sciences, University of Michigan, Ann Arbor, Michigan 48109; lmwalter@umich.edu*

Lynn M. Walter received her M.S. degree from Louisiana State University (1978) and her Ph.D. from the University of Miami (1983). She was an assistant professor at Washington University in St. Louis until 1988. She then joined the University of Michigan, where she is now a professor of geological sciences and director of the Experimental and Analytical Geochemistry Laboratory. Her research interests focus on the hydrogeochemistry of near-surface and deeper basin environments, with emphasis on carbon transformations and mineral mass transport.

Datashare 32

Five supplementary tables are accessible in an electronic version on the AAPG Web site (www.aapg.org/datashare) as Datashare 32.

central to northern Uinta Basin. Here, the organic-rich, immature Green River shales experience meteoric water invasions and formation fluid chemistry, and stable isotope compositions are diagnostic of microbial methanogenesis.

INTRODUCTION

Tertiary intermontane basins in the Rocky Mountain region have hosted more discoveries of natural gas fields in the last 10 yr than most other major onshore provinces in the United States (e.g., Law and Curtis, 2002; Schmoker, 2002). Gas is the fastest growing component of world energy, with consumption in 2020 projected to double the 1999 total (e.g., Schmoker, 2002), so identifying reserves from both conventional and unconventional resources has gained momentum. Conventional resources are buoyancy-driven deposits, occurring as discrete accumulations in structural and/or stratigraphic traps, whereas unconventional resources (e.g., coalbed methane [CBM], shale gas, and basin-center or deep gas) are regionally pervasive and mostly independent of structural and stratigraphic traps (e.g., Law and Curtis, 2002; Shurr and Ridgley, 2002). The origin of natural gas in these accumulations may be from thermogenic sources (either from primary cracking of organic matter or secondary cracking of bitumen and oil into gas) or from a mix of thermogenic-biogenic sources. Moreover, in these same basins, formation waters of high salinity have been observed (e.g., Holmes, 1985; Wanty et al., 1991; Gwynn, 1992, 1995; Dyni, 1996). Such high-salinity waters were commonly studied in localized settings restricted to a few formations. When evaluated at regional scales, data coverage was sparse and typically lacking information on minor elements and stable isotopes. However, without these measurements, the origin and extent of deep saline fluids in these basins remain poorly understood.

A significant body of work documents the origin of biogenic and thermogenic hydrocarbon gases and high-salinity formation waters in sedimentary basins (e.g., Walter et al., 1997; Martini et al., 1998, 2003). In particular, McIntosh et al. (2004a, b) and McIntosh and Walter (2005) showed that the integration of gas and water stable isotope relations with regional patterns of salinity acquisition can be used to understand basin-scale hydrodynamics and to improve the exploration and recovery of unconventional gas resources. For example, along the shallow margins of the midcontinent basins, the geochemistry of formation waters associated with microbial gases reveals important links to gas genesis. These links

distinguish the methane-rich microbial gases from purely thermogenic sources, i.e., negative $\delta^{13}C$ in methane and positive $\delta^{13}C$ in CO_2 and dissolved inorganic carbon (DIC) point to methanogenesis (Scott et al., 1994; Shurr and Ridgley, 2002; McIntosh et al., 2004a, b). By further evaluating formation water $\delta^{18}O$, δD (deuterium isotope ratio), salinity, as well as methane δD, the timing of freshwater recharge, its potential migration pathways, and the association to gas genesis can be inferred.

In this study, the hydrocarbon-rich and spatially delimited Cretaceous–Tertiary (K-T) section of the Uinta Basin in Utah, coupled with excellent access to data and sampling from active drilling programs, provides an ideal opportunity for an integrated, regional-scale study of formation water geochemistry, gas geochemistry, and regional hydrodynamics. Both conventional and unconventional gas deposits are common in this basin, but the origin and migration of such gases remain poorly understood. For example, at the shallow depths along the basin margin, the extensive coal beds of the Mesaverde Group and the organic-rich shales of the Green River Formation are thermally immature (Nuccio and Fouch, 1992; Tabet and Quick, 2001; Schamel, 2005), providing potential fairways for microbial gas generation. However, these same formations, when deeply buried, are sufficiently mature for thermogenic gas generation, and the development of basin-center deep gases is suggested (Rice et al., 1992; Nuccio and Roberts, 2005). To date, the origin, extent, and distribution of the thermogenic versus biogenic gases in the Uinta Basin are not well understood.
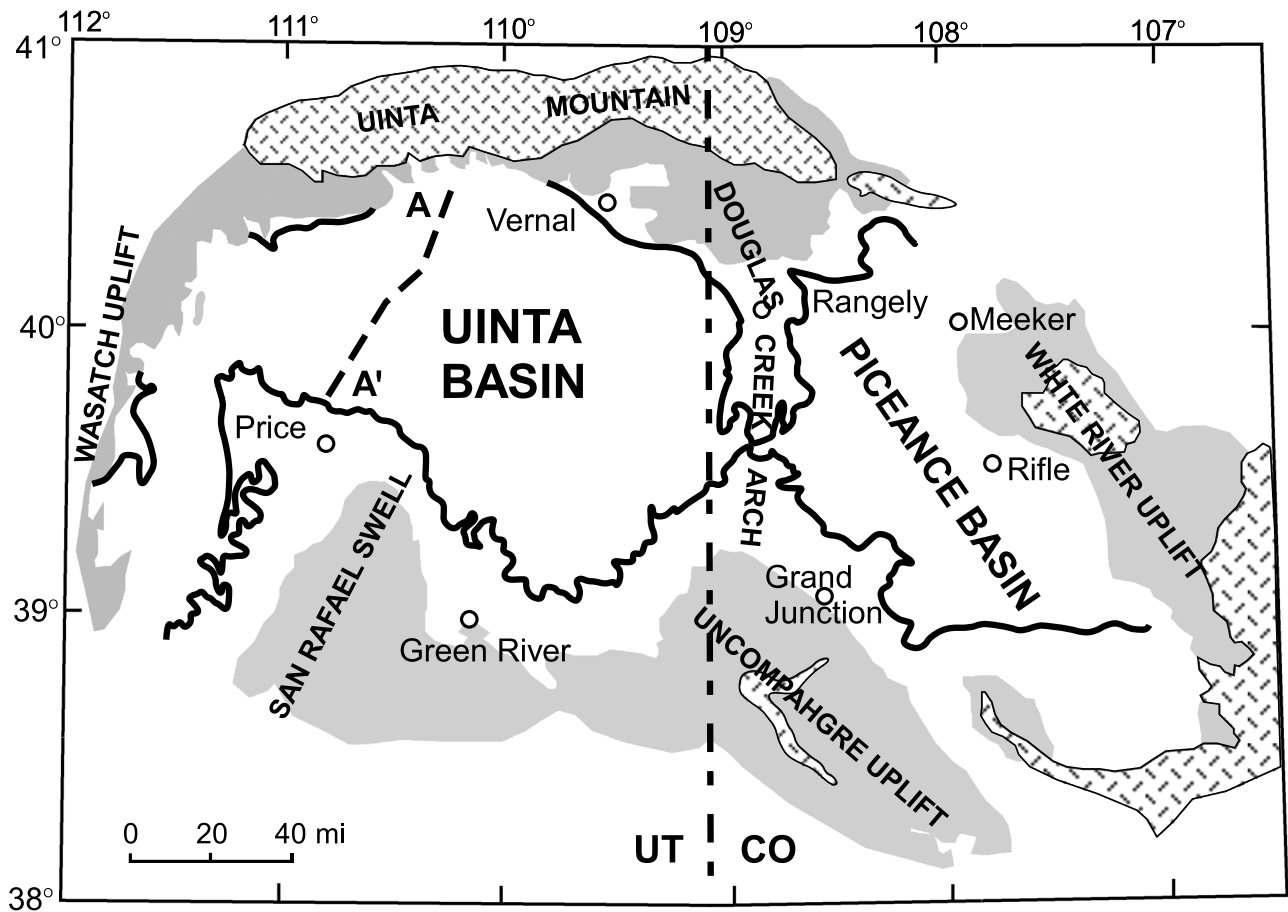
In this study, using water and gas geochemistry data based on sampling and compilation of past records, we investigate the origin of salinity in the relatively young, mostly lacustrine sediments of this basin, which is representative of many intermontane basins in the Rocky Mountain region. To understand gas source rock, genesis and migration, water composition, gas composition, and stable isotope signatures were integrated at the regional scale. Using a hydrostratigraphic model, the compositional data are further mapped in three dimensions to provide evidence in support of long-distance fluid migration.

UINTA BASIN

Geology

Located in northeastern Utah and northwestern Colorado, the Uinta Basin is an east-west–trending intermontane basin within the northern Colorado Plateau (Figure 1). Prior to the basin formation, much of the Rocky Mountain region, including the Uinta Basin, was covered by an epicontinental sea where deposition lasted from about 100 to 83 Ma (Howells et al., 1987). The end of this marine deposition is generally marked by the deposition of the Mesaverde Group. The basin was created during the Laramide orogeny (Late Cretaceous through Eocene, 75 to 50 Ma), within the rapidly subsiding Lake Uinta (Picard, 1985). To the north and west of the basin, uplifts of the Uinta and Wasatch Mountains initiated during the Late Cretaceous. The simultaneous subsidence in the basin created depositional environments ranging from alluvial or fluvial to wetland and shallow lacustrine. South of the basin, the San Rafael swell and the Uncompahgre uplifts began during the late Campanian and continued until late Eocene. These uplifts are likely responsible for the gentle dip of the southern basin (McPherson and Bredehoeft, 2001). During the Tertiary, these highlands and uplifts surrounding the basin provided much of the sediment sources to the basin. In the last 10 m.y., the basin has experienced regional uplift associated with the development of the Colorado Plateau, resulting in the erosion and removal of about 1 km (0.6 mi) of Oligocene and Eocene rocks (Pitman et al., 1982).

Today, the basin is both a structural and topographic basin. The basin is structurally asymmetrical to the north where the basin axis is approximately aligned east–west. Strata north to the axis dip steeply toward it, whereas those south of it dip generally toward it. The deepest strata thus lie in the northern one-third of the basin where several prolific hydrocarbon reservoirs are located (discussed in the section titled Hydrocarbon Plays). Although the basin contains about 10 km (6.2 mi) of sedimentary rocks ranging in age from late Precambrian to Oligocene (Anders et al., 1992), this
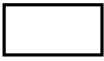
Figure 1. Uinta Basin location (modified from Johnson and Flores, 1998). K-T = Cretaceous–Tertiary.

study focuses on the Upper Cretaceous and Tertiary section only (upper 5–7 km (4.3 mi) of the sedimentary sequence), corresponding to the terrestrial history of the basin. This section is also where most of the water and hydrocarbon database are located. Major geological formations include the Duchesne River Formation, Uinta Formation, Green River Formation, Wasatch Formation, and Mesaverde Group (see Figure 2, which includes a representative cross section and a stratigraphic column). The Mancos Shale, which underlies the Mesaverde Group, is a regionally important aquitard. However, despite significant hydrocarbon productions

from this unit, water chemistry data are generally sparse. This unit is thus not emphasized. Hydrogeologically, these formations constitute either aquifers or aquitards, producing a multilayered aquifer system at the regional scale (Glover et al., 1998).

In terms of lithology, the major formations are composed of sandstone, siltstone, coal, shale, limestone, and dolomite deposited in fluvial, deltaic, and lacustrine environments (Fouch, 1975). The Duchesne River, Uinta, and Wasatch formations consist of sandstone, siltstone, claystone, and conglomerates created in fluvial to alluvial environments. The Green River Formation, however, contains two
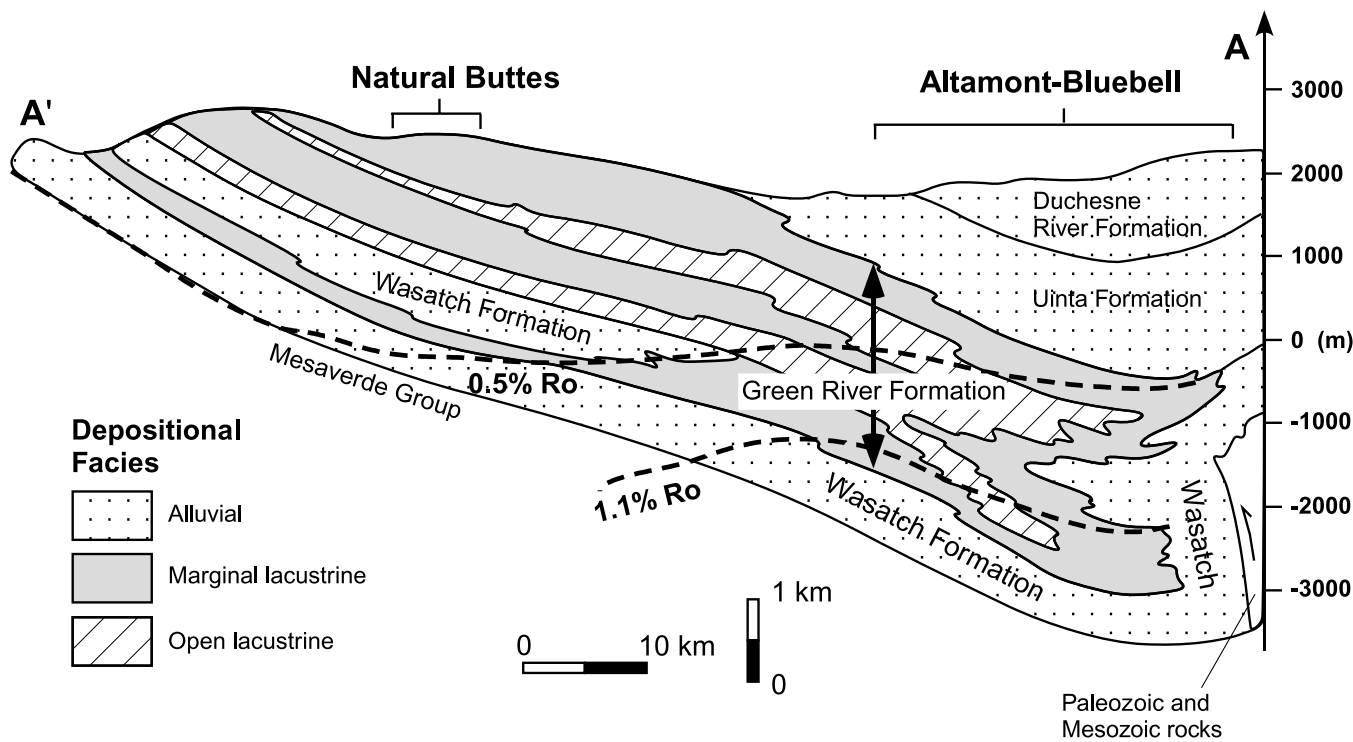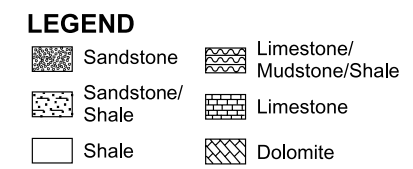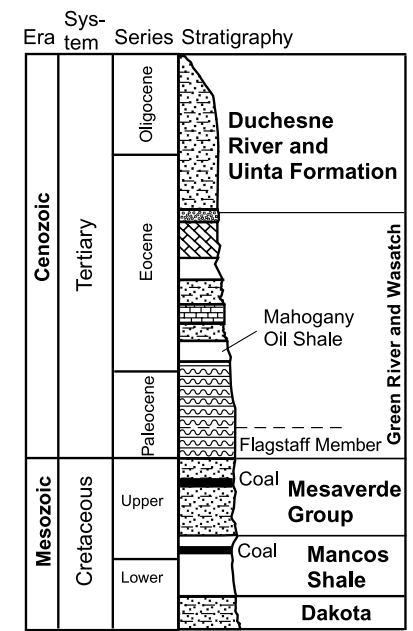
Figure 2. A northeast-southwest–trending cross section (AA') with major Cretaceous–Tertiary (K-T) formations and associated depositional environments (from Fouch, 1975). Two contours of vitrinite reflectance are shown indicating the estimated thermal maturity of the sediment organic matters (Fouch et al., 1994). The location of AA' is indicated in Figure 1. Stratigraphy, including the major lithology, is also shown (from McPherson and Bredehoeft, 2001; USGS, 2002).

dominant facies (Figure 2): an open-lacustrine organic-rich shale and carbonate facies, which acts as hydrocarbon source rocks when deeply buried, and a marginal lacustrine sandstone, claystone, and carbonate facies, which acts as hydrocarbon reservoirs or cap rocks. The facies positions are complex and interbedded, reflecting the changing boundaries and the cyclic rise and fall of the lake level during basin filling (Surdam and Stanley, 1980; Fouch et al., 1994). Because rocks that compose the Mesaverde Group were deposited in a coastal to marginal marine environment during the time when the sea level varied, the lithology of this group varies vertically and laterally and intertonguing is common (Robson and Banta, 1995).

In terms of bulk mineralogy, the Duchesne River and Uinta formations have similar lithology and hydrologic properties (Naftz, 1996) and are commonly studied as a single hydrogeological unit (the Duchesne-Uinta aquifer) (Glover, 1996). They contain minerals such as quartz, calcite, plagioclase, biotite, and clay minerals (Naftz, 1996). The Green River Formation has been much studied because of its hydrocarbon significance. It contains quartz, feldspar, halite, sodium bicarbonate, anhydrite, and authigenic clay minerals and carbonates (calcite, dolomite, and ankerite) (e.g., Pitman et al., 1982; Wanty et al., 1991; Fouch et al., 1994; Dyni, 1996), in addition to various organic materials (e.g., kerogen, bitumen, and gilsonite). The evaporite minerals in this formation are commonly associated with kerogen-rich shales, indicating codeposition during periods of closed hydrological condition with high organic productivity (Fouch et al., 1994). The Mesaverde Group contains quartz, feldspar, sulfate evaporites, and authigenic minerals (quartz, calcite, dolomite, ankerite, and clay minerals), along with organic materials (possibly kerogen) and coal (Pitman et al., 1982, 1988).

Hydrogeology

In the Uinta Basin, within the upper Tertiary deposits, the combination of high relief and high precipitation rates along the basin margin compared to the basin interior has produced an active, regional-scale topographically driven groundwater flow system (Willett and Chapman, 1987; Glover, 1996, Glover et al., 1998) (Figure 3a, b). Regional groundwater recharges along the uplifted basin margins and discharges into the Green River and its tributaries in the central basin. Because of the higher elevation and cooler surface temperature of the Uinta Mountains, approximately 80% of the total groundwater recharge occurs in the northern basin (USWP, 1999). As a result, groundwater circulates throughout these deposits in the northern basin, creating significant geothermal anomalies at the regional scale (Willett and Chapman, 1987, 1989; Zhang et al., 2005). Vitrinite reflectance modeling further suggests that the present geothermal anomalies (and thus regional groundwater flow system) may have existed for millions of years (Willett and Chapman, 1987).

However, hydrogeology of the deeper basin is significantly influenced by regional-scale fluid overpressures, particularly in the deeply buried lower Green River Formation in the northern basin, at the Altamont-Bluebell oil field. Here, fluid pressures approach lithostatic, likely induced by hydrocarbon generation (Spencer, 1987; Fouch et al., 1992; Bredehoeft et al., 1994). Figure 3c shows the observed hydraulic head of the Flagstaff Member of the basal Green River Formation (McPherson and Bredehoeft, 2001). Such high heads may act as barriers for the deeper groundwater flow, whereas fluid movement outside this zone is likely outward, away from the observed overpressures. Moreover, the hydraulic head of the Mesaverde Group, wherever it is available, is normal to subhydrostatic (as indicated by values lower than the surface elevation of the basin) (Figure 3d). This is likely the result of hydrocarbon gas saturation because the gas column has a significantly lower density than water even under in-situ conditions (this phenomenon was also hypothesized for the underpressured parts of the Arkoma and Appalachian basins) (Ingebritsen et al., 2006). However, hydraulic data on the Mesaverde Group are sparse in the deeply buried central regions of the basin (Figure 3d), whereas some evidence suggests that the upper part of this group may be slightly overpressured, possibly because of gas generation from the interbedded carbonaceous
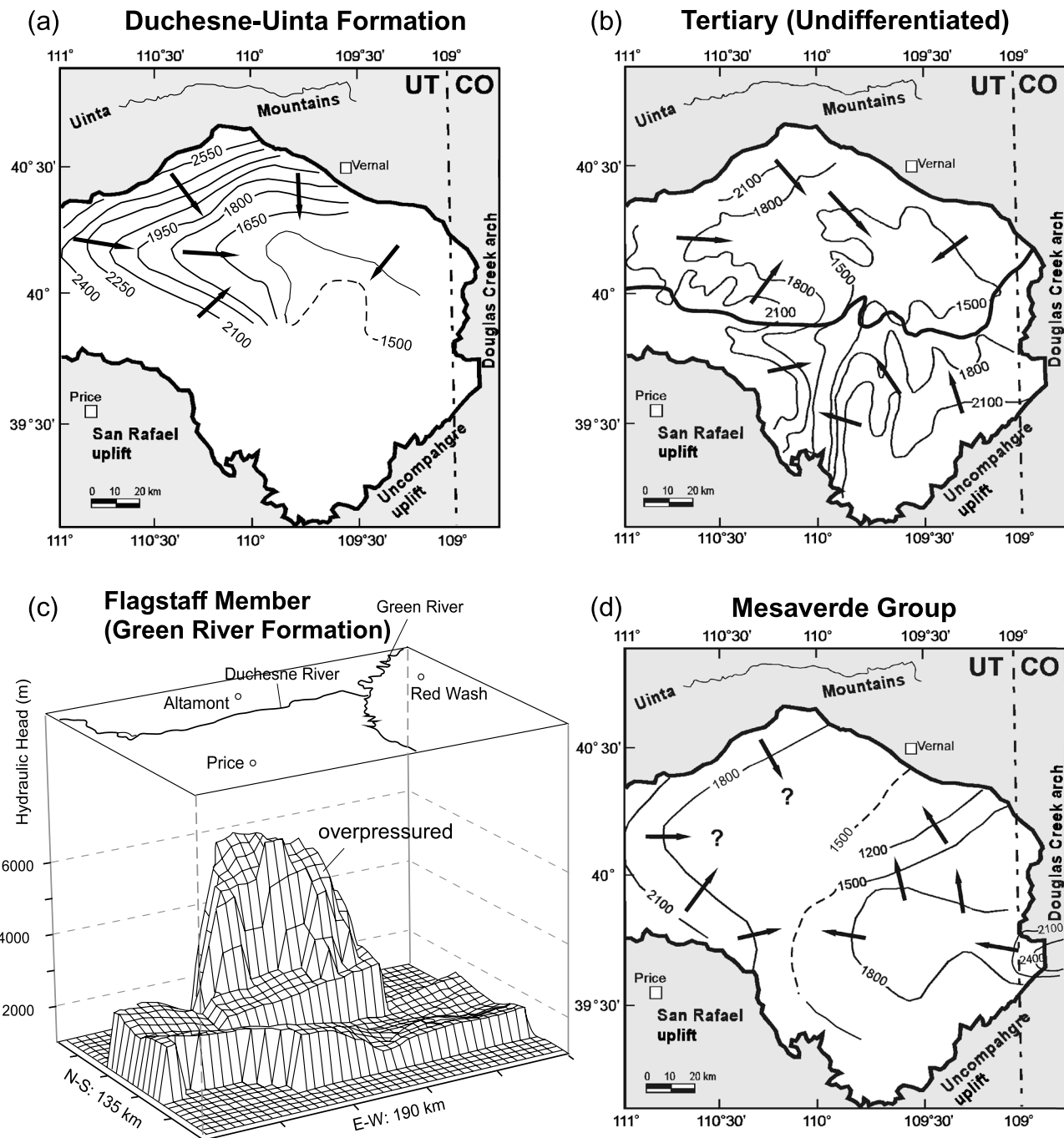
Figure 3. (a) Observed potentiometric surface (m) of the Duchesne-Uinta aquifer (from Glover, 1996) with the inferred groundwater flow directions (arrows). (b) Observed potentiometric surface of the undifferentiated Tertiary formations (from Holmes, 1985). In the southern basin, the hydraulic head corresponds to that of the Green River and Wasatch formations (the bold curve marks the southern extent of the Duchesne-Uinta aquifer). (c) Observed hydraulic head of the Flagstaff Member of the lower Green River Formation (from McPherson and Bredehoeft, 2001). At the Altamont-Bluebell field in the northern basin, the Flagstaff head is much higher than surface elevation (1.5–2.5 km [0.9–1.5 mi]), indicating fluid overpressure. (d) Observed potentiometric surface of the Mesaverde Group (from Freethey and Cordy, 1991; Robson and Banta, 1995). Areas without contours are because of lack of data; the dashed line indicates large uncertainty.

source rocks and coals (Pitman et al., 1982). Thus, the nature of hydrocarbon gas in this formation is uncertain.

In the Uinta Basin, the total dissolved solids (TDS) of the formation waters generally increase from the recharge areas toward the discharge areas

(Holmes and Kimball, 1985; Howells et al., 1987; Freethey et al., 1988; Naftz, 1996). In the Duchesne-Uinta aquifer, dominant water-rock reactions include plagioclase dissolution (and associated kaolinite precipitation), Na-Mg and Na-Ca cation exchange, and carbonate dissolution (Naftz, 1996). In the Green River and Wasatch formations, reactions include evaporite dissolution, feldspar dissolution (and associated clay mineral formation), and carbonate precipitation (Wanty et al., 1991). Along the regional groundwater discharge areas (i.e., Green River Valley in the central basin), formation water chemistry becomes dominantly Na-Cl type (Wanty et al., 1991). This cannot be explained by simple projection of water-rock reactions from the recharge areas because geochemical flow-path modeling of the formation water compositions indicates that a substantial addition of extra NaCl is needed to account for the observed water chemistry (Wanty et al., 1991). Furthermore, beneath the discharge areas, these water samples were taken over a large sampling interval from 0.3 to 1.9 km (0.18 to 1.1 mi), suggesting the existence of an extensive vertical NaCl plume. In the central Uinta Basin, the upwelling of deep saline formation waters was indeed suspected, with evidences including the existence of saline springs, thermal anomalies (warm springs), and hydrocarbon correlations (M. Szpakiewcz, 2006, personal communication). However, other salt sources cannot be entirely ruled out, especially at shallow depths, because of, for example, irrigation return flow or dissolution of local evaporites by shallow groundwaters (USWP, 1999). Thus, within the Uinta Basin, large uncertainties exist in the sources of high salinity observed near the surface, in shallow aquifers and springs along the discharge areas (Holmes, 1985; Wanty et al., 1991).

Hydrocarbon Plays

Numerous oil and gas fields exist in the Uinta Basin, originating from the open lacustrine limestones and shales of the Green River Formation and marginal lacustrine organic-rich sandstones and shales of the Mesaverde Group and Mancos Shale (Fouch et al., 1992; Ruble et al., 2001; Longman, 2003; Chidsey et al., 2005) (Figure 4). Most oil in the basin is produced from the greater Altamont-Bluebell field where fluid pressures approach lithostatic, likely induced by hydrocarbon generation. This field is considered a typical example of deep-basin overpressured hydrocarbon systems (Lucas and Drexler, 1975; Spencer, 1987). Solution waters have been analyzed for dissolved light hydrocarbons from this field as well as the Pariette Bench field to the south (Zhang et al., 2005). Significant concentrations of dissolved BTEX (benzene, toluene, ethylbenzene, and xylene) were discovered, indicating waterwashing of the oil pools. Using a coupled fluid flow, heat transfer, and solute transport model, which was calibrated to observed regional hydraulic head, temperature, and downhole pressure at the Altamont-Bluebell, sources of these waters were modeled in this early study as meteoritic recharge from the northern Uinta Mountains. Furthermore, numerous gilsonite veins exist in the northeastern basin. Fluid inclusion studies suggest that they were sourced from the overpressured section of the Green River Formation in the northern basin (Monson and Parnell, 1992). The gilsonite veins were solid hydrocarbons formed after migrating into fracture zones opened by overpressure.

Unconventional (continuous type) natural gas plays have also been identified (Schmoker et al., 1996; USGS, 2002), some associated with oil production (e.g., gases produced from the Altamont-Bluebell and Red Wash oil fields), but most are nonassociated (e.g., the Natural Buttes gas field). These plays have characteristics of basin-center gases, including low matrix permeability, areally large deposits, and lack of obvious traps or seals.

The vitrinite reflectance (R_o) of the sediment organic matters (Fouch et al., 1994) indicate that, in the northern basin, the deeply buried sections of the Green River Formation fall within the oil window ($0.5–1.1\%R_o$, Figure 2), coinciding with the observed interval of oil generation in the Altamont-Bluebell field. However, in the central to southern basin where the Green River Formation is much shallower, the organic-rich facies (open lacustrine in Figure 2) are thermally immature for oil generation.
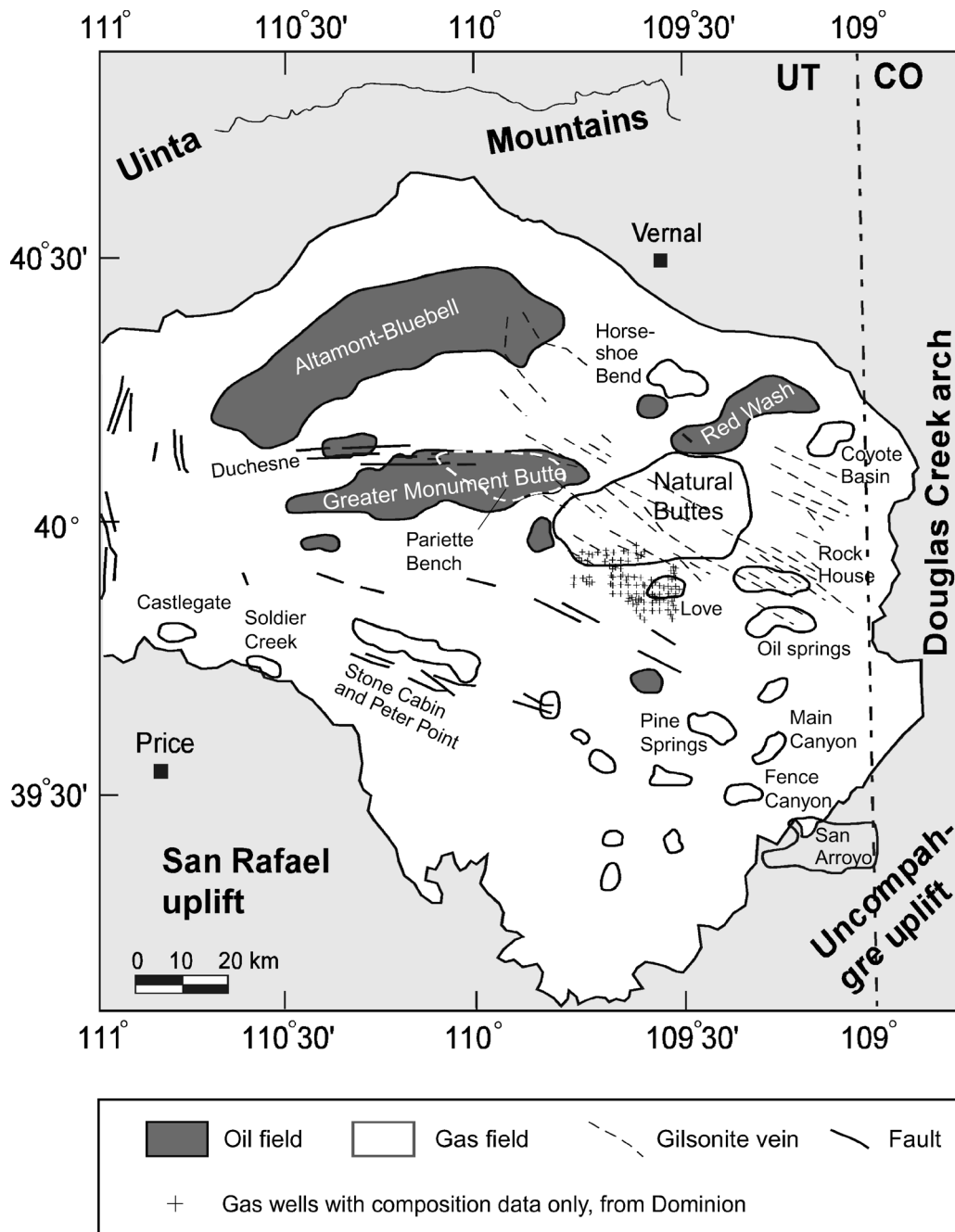
Figure 4. Major hydrocarbon-producing fields in the Uinta Basin along with the observed faults and gilsonite veins (from Fouch et al., 1994; Longman and Morgan, 2008). Locations of the Dominion gas wells (where compositional data are available) are superimposed.

Similarly, in the northern basin, the deeply buried Mesaverde Group has R_o falling within the gas window (1.1–3 %), indicating that its maturity is optimal for gas generation (Nuccio et al., 1992; Johnson and Flores, 1998; Nuccio and Roberts, 2005). A large gas reserve has thus been estimated (USGS, 2002). However, at the Natural Buttes gas field, the reservoir rocks (dominantly Wasatch and Mesaverde) fall outside the gas window (Fouch et al.,

1992), suggesting that gases produced from this field are generated elsewhere, possibly from the deeply buried Mesaverde Group in the northern basin. However, without detailed composition and isotope data on both produced gases and associated formation waters, the mechanisms responsible for the origin, genesis, and migration of such gases are unclear.

The present investigation focuses on the non-associated gases produced from the Natural Buttes
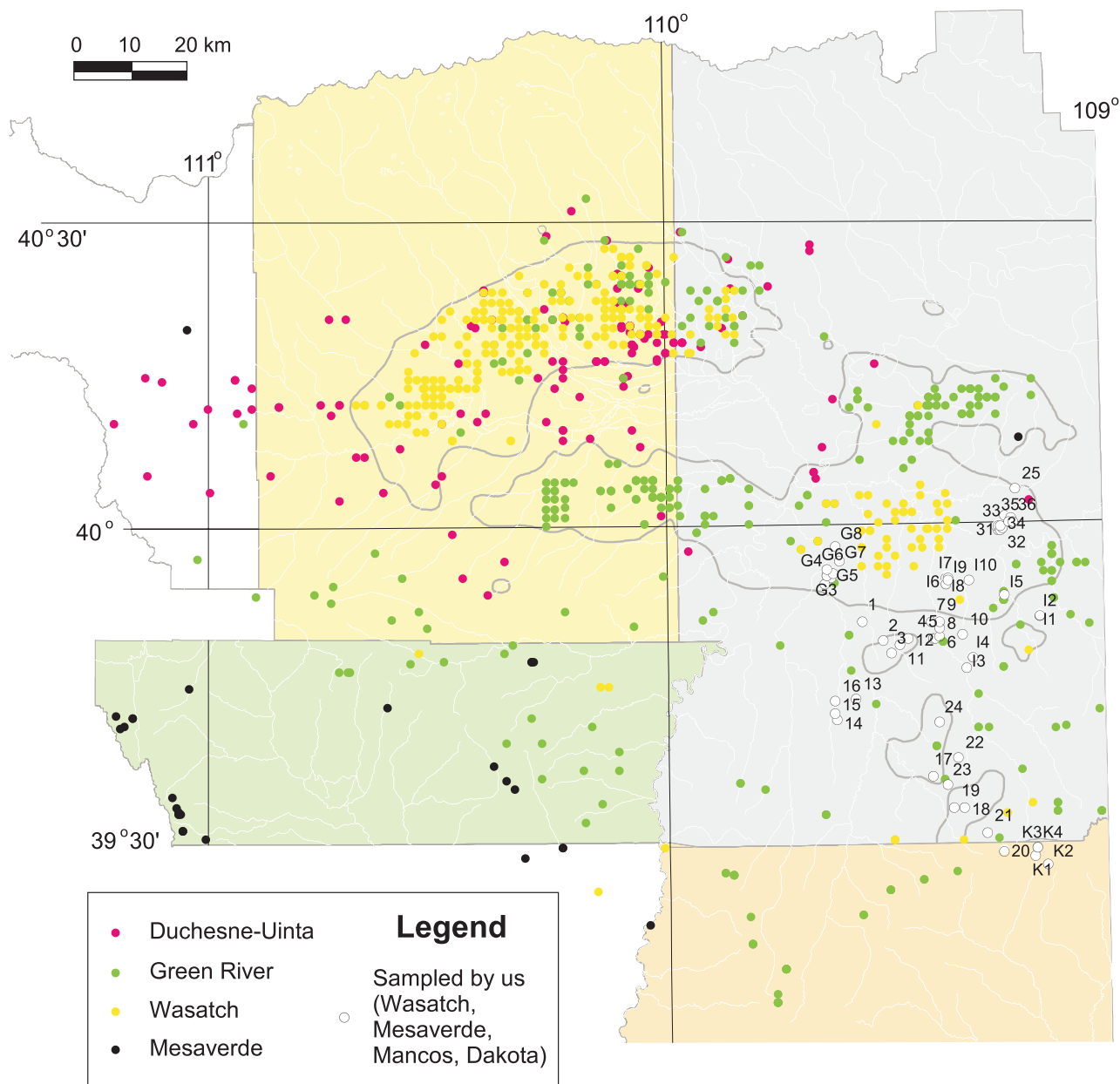
Figure 5. The Geographic Information System (GIS) county map superimposed with the location of wells of this study. Major oil and gas fields (gray outlines) are also shown. Wells sampled in this study are shown as black empty circles, each with an ID tag (full well name is listed in Table 1; see AAPG Datashare 32, www.aapg.org/datashare). The location of preexisting water geochemistry data is shown as colored dots, grouped for the individual geological formation.

gas field and its vicinity as well as those of the smaller gas fields in the southeastern basin. Two potential sources and migration pathways were proposed for the Natural Buttes gases: (1) southward migration of deep thermogenic gases from the Altamont-Bluebell field (source: type I kerogen) (Rice et al., 1992); (2) in-situ production of thermogenic gases from the deeply buried Mesaverde

Group (source: type III kerogen) (Osmond, 1990; MacMillan, 1997). Gas migration from the Natural Buttes toward the immature Mesaverde coal beds along the southeastern basin was also suggested (Tabet and Quick, 2001). This pathway is opposite of the regional hydrodynamic drive (Figure 3), raising the interesting issue of water-gas interaction and fluid expulsion at the regional scale.

In this study, gas wells were sampled from the Natural Buttes gas field (regional groundwater discharge area) toward the southeastern basin margin (regional recharge area) (Figure 5). At the Natural Buttes gas field, industry sources provided gas composition data, which allow a detailed comparison with our sampled gases. The smaller gas fields to the southeast of Natural Buttes are recent exploration targets, providing direct access to new formations and depths. Here, most of the wells perforate the Wasatch Formation and the Mesaverde Group (a few in the Mancos Shale and Dakota Formation), providing access to the gas-producing formations in the southeastern basin, which have heretofore been unavailable.

Existing Records

An extensive water chemistry database of the major Tertiary formations has been assembled from the U.S. Geological Survey, Utah Geological Survey, and Utah Department of Water Resources (Gwynn, 1995; J. W. Gwynn, 2006, personal communication; B. Kimball, 2006, personal communication; USGS, 2009). An original record of about 2000 wells was obtained, containing major element data of water samples collected from domestic wells, springs, and oil-gas production and test wells. From this record, a screening analysis was conducted first to remove spurious or incomplete data. This included eliminating wells with ionic charge imbalances greater than 5%; and wells with incomplete location and perforation information. For the oil and gas wells, only production wells were retained. A final filtered database of 844 wells, which provides spatial and depth coverage of water geochemistry at the basin scale (colored dots in Figure 5), was obtained.

For each well, information on latitude, longitude, elevation, and sampling depth is available. However, most of the water chemistry consists only of the major elements (i.e., Na, Ca, Mg, Cl, HCO_3, and SO_4). With a few exceptions, minor elements and stable isotope data are not reported. Most wells are further limited to sampling the Tertiary formations; their locations are clustered around the major producing fields. Thus, data coverage

on the lower Tertiary to Cretaceous formations (e.g., Mesaverde Group) is sparse or nearly absent, particularly in the southeastern basin (Figure 5). In this study, the field fluid sampling program filled an important void in this region. Furthermore, our complete suite of analysis provides a means of integrating minor element and stable isotope data into this existing record.

A hydrocarbon gas database of the basin was also compiled from published and private sources. According to Rice et al. (1992), composition and stable isotope data were available for 23 wells, including nonassociated Natural Buttes gases and associated gases of the Altamont-Bluebell and Redwash oil fields. However, these records pertain to older wells for which detailed location information is either incomplete or absent. Data from the Dominion Gas Company consist of 217 gas wells with complete location and perforation information. However, these data were sampled from limited areas within and south of the Natural Buttes gas field (Figure 4), and only compositional analysis is available. Finally, neither records have information on the geochemical makeup of the coproduced formation waters. These limitations were addressed in this study by conducting a regional-scale sampling and analyses of gases and coproduced waters. In the following sections, the existing records will be analyzed and integrated with key new data obtained from field sampling.

METHODS AND RESULTS

Three energy companies active in the Uinta Basin offered critical field assistance with their well operators. During the summers of 2006 and 2007, 56 gas wells were sampled for hydrocarbon gases and coproduced formation waters, along a general transect from the Natural Buttes gas field toward the southeastern basin (Figure 5). In selecting wells, production wells providing both spatial and depth coverage were identified wherever possible (Table 1, see Datashare 32, www.aapg.org/datashare). In some locales where multiple wells were available, those with the narrowest perforation intervals were selected for better spatial control. Because of

production practices, most of the water samples had to be obtained from separator tanks instead of wellheads. However, the tanks were all flushed recently ahead of fluid sampling to obtain the most representative samples possible, thus most tanks held freshly collected formation waters. All gases were collected at wellheads. Most wells were producing gases, although a few produced waters rich in hydrocarbon liquids. The protocols used to sample and analyze the coupled formation waters and gases can be found in our previous work (Martini et al., 1998, 2003; McIntosh et al., 2004a, b).

All water samples were analyzed for geochemistry, providing a high-quality data set, including major and minor elements. A select subset of 23 wells were additionally analyzed for (1) stable isotopes of coproduced waters ($\delta^{18}O_{H_2O}$, δD_{H_2O}), (2) $\delta^{13}C_{DIC}$ of DIC, and (3) gas composition and stable isotopes ($\delta^{13}C_{CO_2}$, $\delta^{13}C_{CH_4}$, δD_{CH_4}). Results of water geochemistry are presented in Tables 2 and 3 (AAPG Datashare 32). Results from the subset are presented in Supplemental Tables 4 and 5. In the following section, these results will be interpreted based on the combined water and gas databases created from the wells sampled in this study and the existing records.

INTERPRETATIONS AND DISCUSSIONS

Formation Water Geochemistry

Major Elements

Formation water TDS in the basin ranges from the very fresh to maximum TDS of 80,000 mg/L, more than twice the salinity of sea water (Figure 6). TDS values do not generally increase with depth, e.g., the Wasatch Formation at depths greater than 8000 ft (2438.4 m) is commonly fresher than the overlying Green River Formation. This may be explained by deep penetration of fresh meteoric waters into the northern basin. At depths between 4000 and 8000 ft (1200 and 2400 m), the Wasatch Formation (deposited in marginal lacustrine and fluvial environments) is interbedded with the Green River Formation (Fouch, 1975; Fouch et al., 1992). In this case, the TDS of the two formations are sim-

ilar, suggesting lateral fluid mixing along equivalent intervals. The TDS versus depth, when compared to the depth plots of the major elements (Figure 6), further reveals the regional importance of Na-Cl type waters. The molarity of Na and Cl reaches up to 1400 mM, whereas the molarity of HCO_3 and SO_4 is of smaller magnitude, as also for Ca and Mg (not shown). However, fresher waters are found in the shallow Duchesne-Uinta aquifer and the Green River Formation (where it outcrops in the southern basin). As depth increases, some deeper Duchesne-Uinta wells sampled increasingly higher TDS, suggesting mixing with fluids of the underlying formations. To determine the dominant ions in the high-TDS waters against those with low TDS, TDS is plotted against Na+Cl concentrations (Figure 7). The dissolved solids in the high-TDS waters are dominated by Na-Cl but not so in the low-TDS waters. These fresher waters come from the Duchesne-Uinta aquifer, Mesaverde Group (black dots in Figure 5, from the preexisting record sampling mostly shallow depths), and the shallower Green River Formation. The typical sampling depth is less than 2000 ft (609.6 m).

To further understand the characteristics of the waters among the formations, Piper diagrams of the major element chemistry are constructed. The samples analyzed in this study are superimposed. These diagrams indicate very similar solute sources between the Duchesne-Uinta and shallow (low TDS) Green River Formation, whereas a high affinity can be discerned between fluids sampled in this study and the Wasatch Formation. This is expected because the Green River Formation underlies the Duchesne-Uinta aquifer, whereas the new samples accessed the lower K-T rocks, mostly from the Wasatch and Mesaverde Group (Figure 6). Waters of the Duchesne-Uinta and shallow Green River formations are generally of the Na-Ca-Mg-HCO_3-Cl type (although at lower TDS, the Ca-Mg-HCO_3-type water becomes increasingly dominant), suggesting significant contribution from reactions occurring near the recharge areas, e.g., dissolution of feldspar, dissolution of carbonates, and possibly ion exchange (Ca + Na_2EX = 2Na + CaEX; Mg + Na_2EX = 2Na + MgEX) (Wanty et al., 1991; Naftz, 1996). However, formation
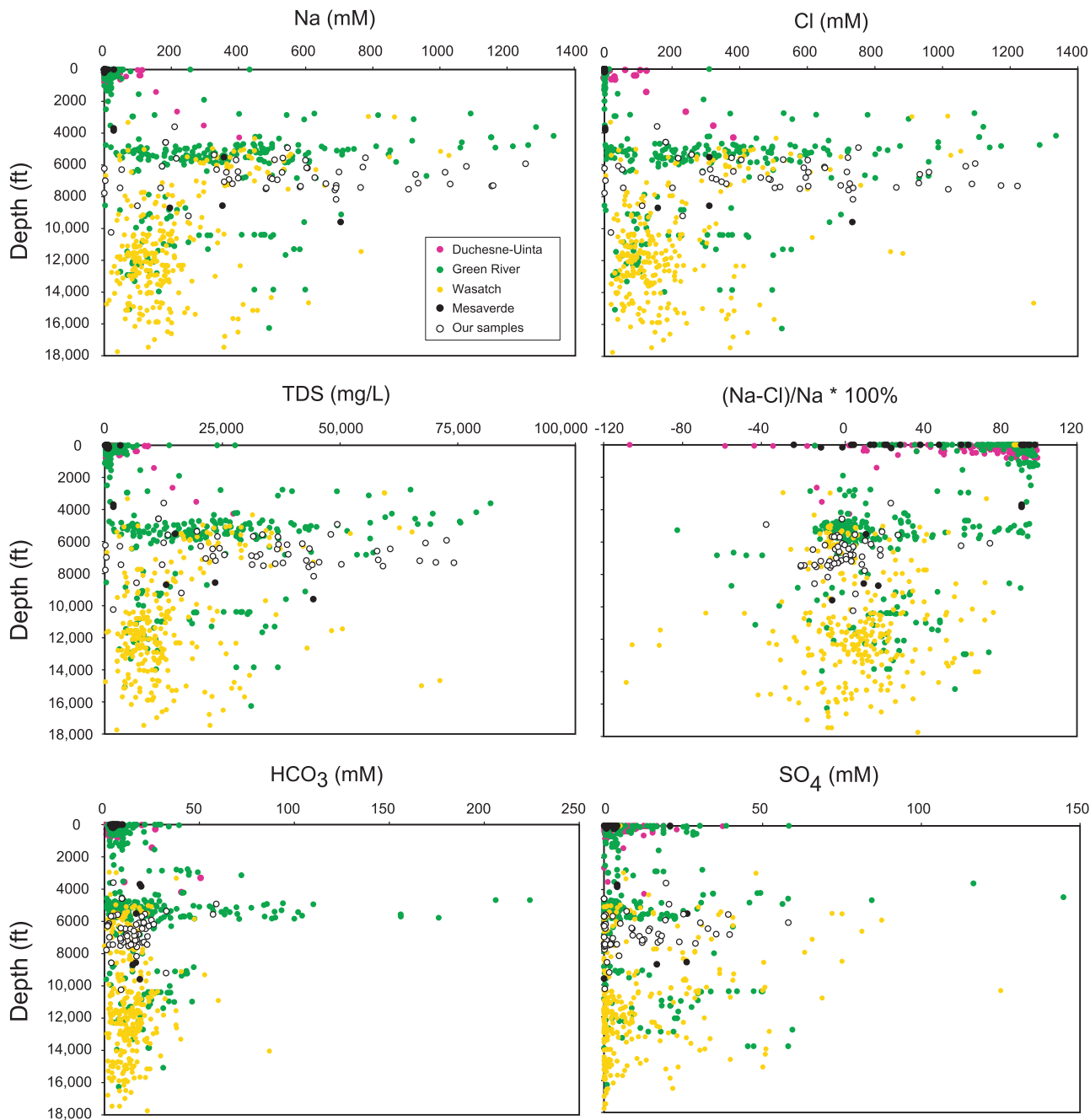
Figure 6. Major element chemistry versus depth for each formation (same color legend as in Figure 5). Wells sampled in this study (black empty circles) access the Wasatch, Mesaverde, Mancos, and Dakota formations in the southeastern basin (Table 1 see AAPG Datashare 32, www.aapg.org/datashare). The sample location for all data is shown in Figure 5. TDS = total dissolved solids; mM = millimolars.

water in the deeper high-TDS flow system (Green River, Wasatch, Mesaverde) is dominated by Na-Cl (Figure 7). This may be explained by the underlying marine shale of the Mancos Group (Duffy et al., 1985; Burtner, 1987) and upward fluid migration (as discussed below).

Crossplots of the major elements provide further insights into the sources of salinity and inorganic carbon. In low-TDS waters, Na versus Cl relations exhibit appreciable scatter around the halite dissolution line (Figure 8a). In such waters, Na is greater in concentration than Cl, indicating

Figure 7. Total dissolved solids (TDS) versus Na + Cl concentrations, in linear (top) and log-log (bottom) scale. At high TDS, the dominant ions are Na-Cl; at low TDS, besides Na-Cl, Ca-Mg-HCO_3-SO_4 make up the rest of the TDS, indicating the influence of fresh recharge waters (see discussions in the text).
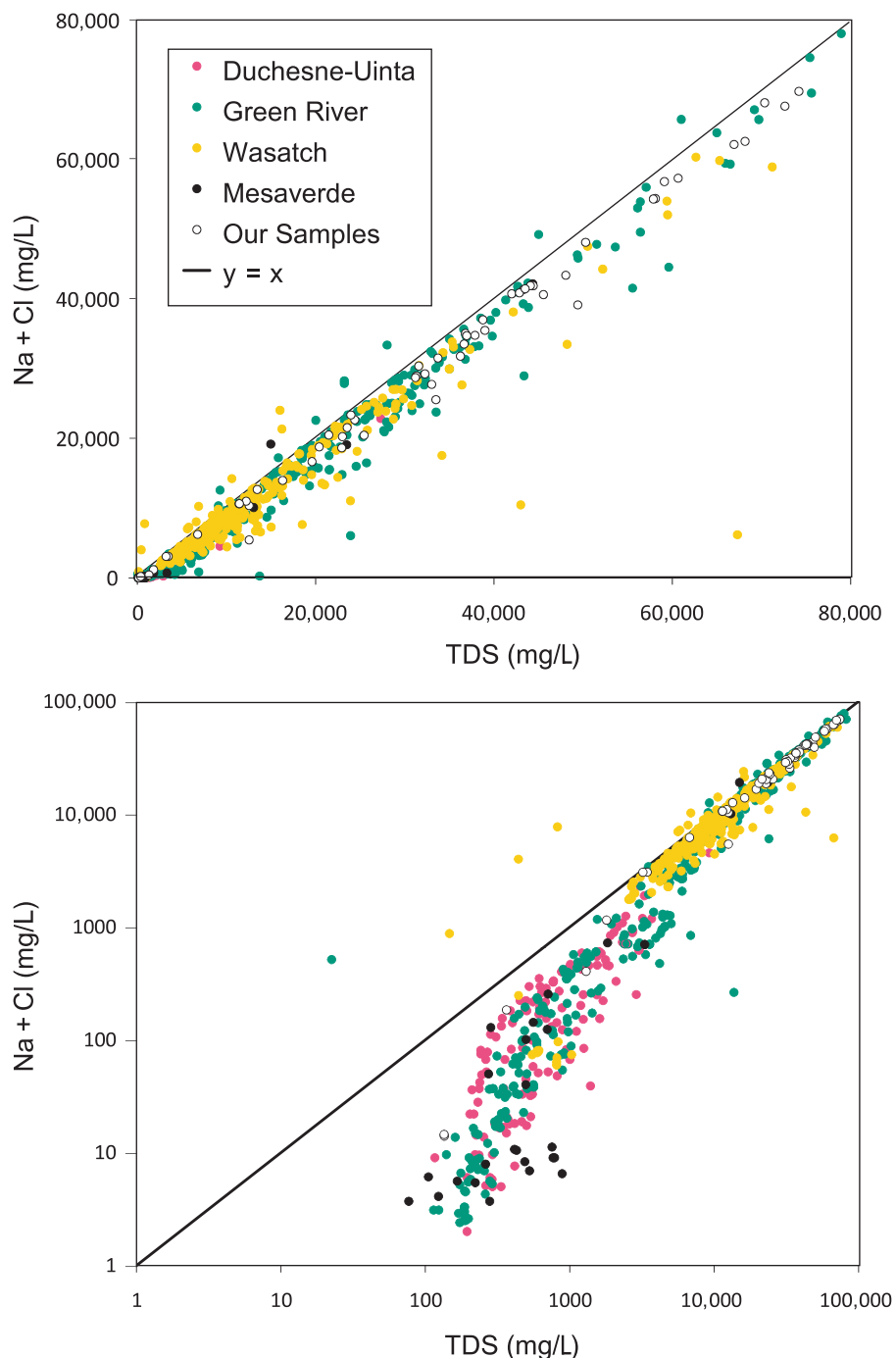
alternative sources. The Na excess, expressed as ([Na]-[Cl])/[Na] × 100%, is especially significant at shallow depths as well as in the deeper Green River Formation, at depths where the HCO_3 concentration is also high (4000–7000 ft [1200–2150 m]) (Figure 6). Because the Green River Formation is known to contain bedded trona ($Na_2CO_3 \times NaHCO_3 \times H_2O$) and nodular nahcolite ($NaHCO_3$) (Dyni, 1996), its Na excesses suggest a likely contribution from evaporite dissolution. The Na excess observed in the Duchesne-Uinta aquifer and the Mesaverde Group (black dots in Figure 5) is likely caused by ion exchange and/or mixing with the Green River waters. This latter possibility will present a genetic relation between sodium excess and HCO_3 concentrations. These formations are thus singled out in plotting Na excess (expressed as [Na]-[Cl]) against HCO_3
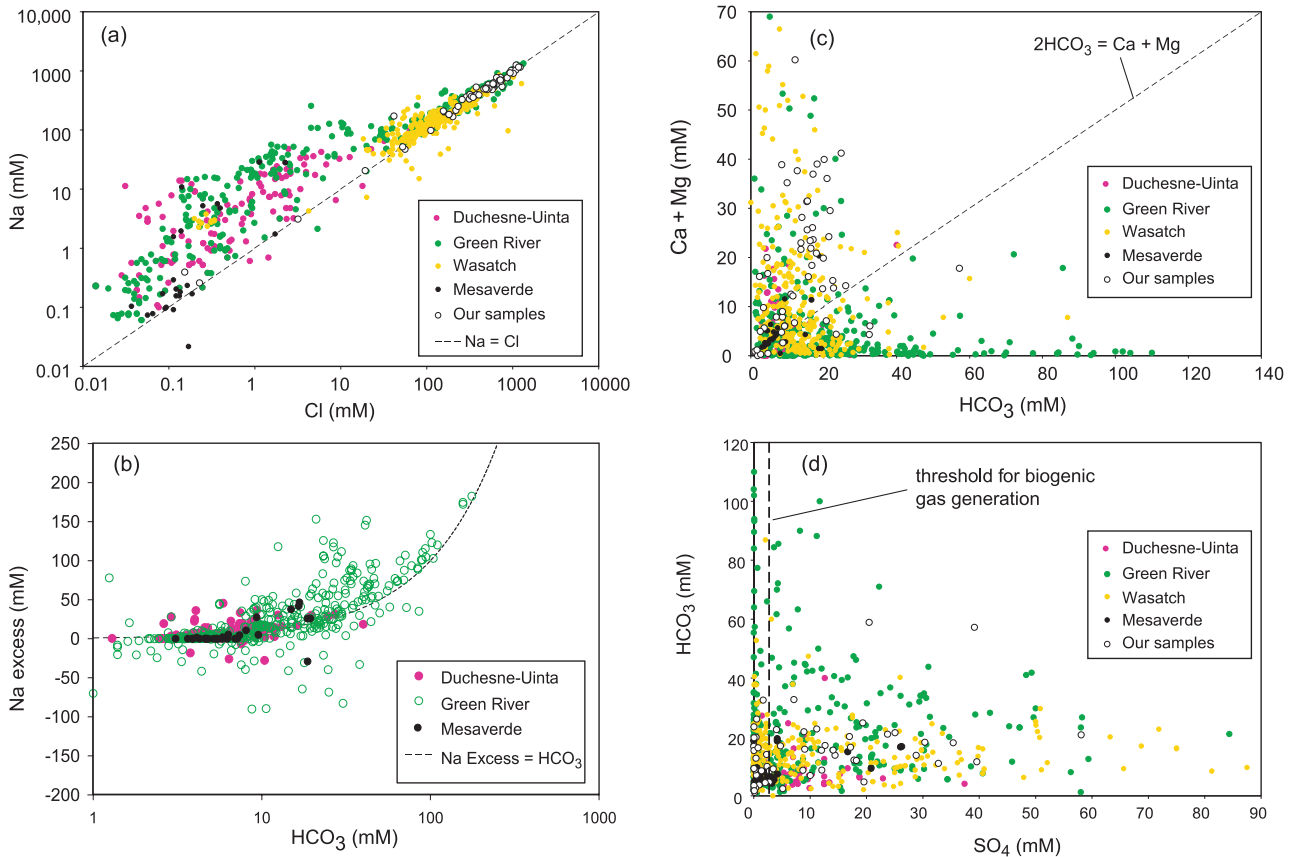
Figure 8. Elemental relationships for the major dissolved constituents of the Uinta Basin formation waters. The Na excess in panel b is defined as [Na]-[Cl] in millimolars (mM).

(Figure 8b). Although significant scatter exists, an appreciable trend is distinguished along the [Na] excess = [HCO_3] line, suggesting that, for many such waters, the extra Na is sourced from the sodium bicarbonate salts. The scattering is likely caused by reactions such as feldspar dissolution, Na-Ca, and Na-Mg exchanges (Naftz, 1996). The exchange reactions can find exchange sites on the regionally pervasive Green River clays. They can also explain the significant Na excess in the low-TDS waters (Figure 8a).

The marginal lacustrine and fluvial Wasatch Formation does not contain significant sodium carbonate and bicarbonate salts. The Wasatch Formation has a molar Na:Cl ratio near 1 (Figure 8a). The Na versus Cl of the new water samples collected in this study closely falls onto the 1:1 trend line (Figure 8a), near the upper end of the salinity range. In the southeastern basin, formation water salinity is exceptionally high despite the relatively

shallow depths of the Wasatch and Mesaverde formations. In particular, their salinity is high compared to the waters of the deeply buried Wasatch Formation in the northern basin (Figures 6, 8a). This is likely caused by freshwater invasion from the Uinta Mountains, which results in the deeper Wasatch rocks being partially flushed.

Because Ca or Mg carbonate mineral solubility can be controlled either by divalent cation variations or DIC variations, the relation between HCO_3 and Ca and Mg is explored (Figure 8c). When viewed basinwide, most data points on Ca + Mg versus HCO_3 fall far from the simple Ca or Mg carbonate stoichiometric dissolution line (2:1 mole relation between HCO_3 and Ca + Mg). This suggests that basinwide, instead of carbonate rock dissolution, most bicarbonate in the formation waters arises either from evaporite dissolution (e.g., trona, nahcolite), microbial methanogenesis (McIntosh et al., 2004a, b), or microbial sulfate

reduction (Carpenter, 1978). However, given the elevated sulfate concentrations observed in these waters (Figure 8d), microbial methanogenesis is not likely. Typically, microbial gas generation only occurs once sulfate has been lowered by microbial sulfate reduction to concentrations below several millimolars (McIntosh et al., 2004a, b). Microbial sulfate reduction is also unlikely because H_2S was not detected in this study nor was it in the study of Szpakiewicz and Collins (1985). This information leads us to believe the likely importance of basin-scale evaporite dissolution in contributing HCO_3 to the formation waters. Note, however, that a significant subset of Green River waters exhibits very low SO_4 (0.01–0.1 mM) and very high HCO_3 (up to 110 mM) (Figure 8d), indicative of gas biogenesis. Upon closer inspection, many come from the central to northern Uinta Basin, sampled at shallower depths from the reservoirs of the Green River Formation, which are known to contain organic-rich shales. As discussed below, gas analysis in this region indeed suggests a biogenic signature.

Minor elements and stable isotopes

Stable isotope compositions provide additional constraints on the origins of solutes and mixing relations of the formation waters. With the exception of well I1, δD and $\delta^{18}O$ values of the samples plot to the right of the global meteoric water line (GMWL) and are far heavier than the modern meteoric water in northeastern Utah (Figure 9). The isotopes of well I1 clearly indicate contamination from surface waters as they fall very close to the modern water line. Also plotted here are waters produced from CBM fields in the Mancos Shale in the southwestern basin (Rice, 2003). Most of the samples in this study fall near the trend line, which extrapolates back toward the GMWL. As discussed by Rice (2003), the fluid end member is isotopically enriched relative to the modern meteoric water. This suggests that the sources of these waters were likely meteoric waters recharged into the basin during the geologic past when the climate was also warmer.

Because evaporation of water produces a greater shift of $\delta^{18}O$ than δD (Clark and Fritz, 1997) and the ancient Lake Uinta was known to produce evap-

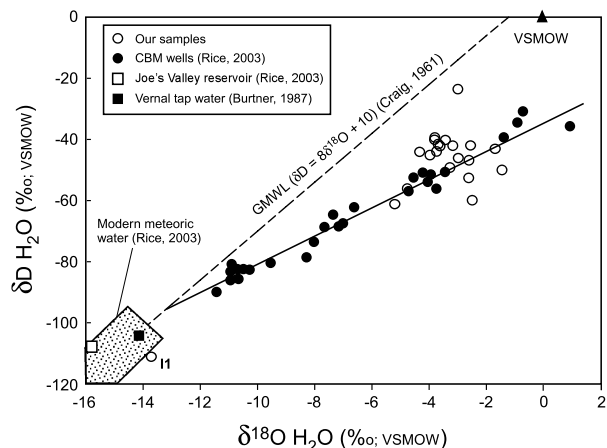**Figure 9.** The δD versus $\delta^{18}O$ of the formation waters sampled in this study (empty circles) along with data analyzed from southwestern Uinta Basin (Rice, 2003) and tap waters in Vernal, Utah (Burtner, 1987). CBM = coalbed methane; VSMOW = Vienna standard mean ocean water.

orite deposits (Surdam and Stanley, 1980), evaporation of formation waters could result in a trend line to the right of the GMWL. This trend line cannot be explained by simple end-member mixing of (ancient) fresh recharge water with marine connate water (near Vienna standard mean ocean water [VSMOW]). Thus, the ancient meteoric waters recharged into the basin must have since evolved, via water-rock reactions along the flow paths, into isotopically heavier formation waters. The formation waters analyzed in this study are thus interpreted to be a mix of evaporatively concentrated seawater with ancient, evolved meteoric water that experienced water-rock reactions.

The above interpretation is supported by variations in the dissolved Br systematics (Figure 10). Bromine is a conservative element (i.e., it generally does not participate in most geochemical reactions in basinal brine systems thus both its concentration and ratios with other conservative element, e.g., Cl, can be used as tracers of groundwater motion) and can be used to determine the mixing relation between basinal brines and fresh water recharged into the basin (e.g., Walter et al., 1990). In Figure 10a, log Cl versus log Br is plotted along the seawater evaporation and dissolution trajectory (Carpenter, 1978). Most of the data have Cl/Br less than that of seawater, short of halite saturation. This suggests that an initial salinity had
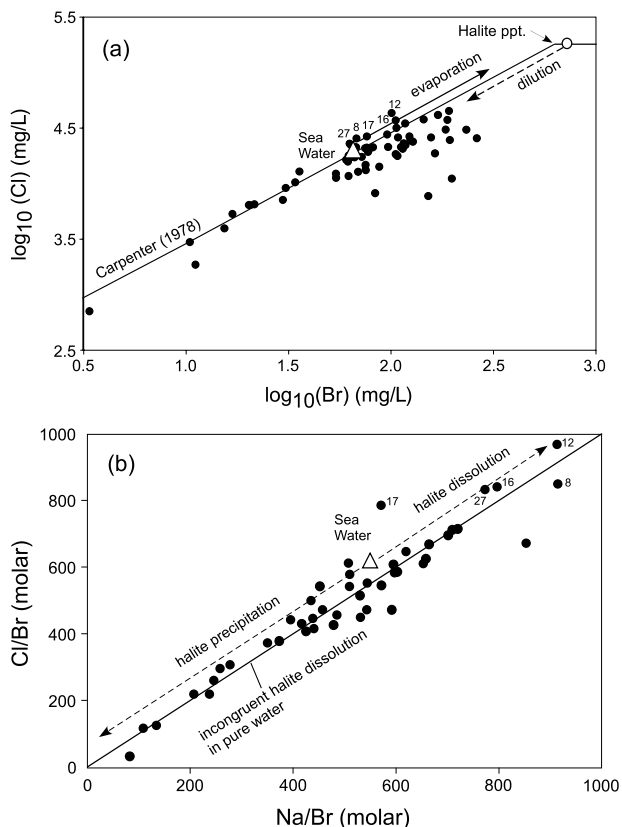
Figure 10. (a) Log Cl versus log Br for the formation waters sampled in this study. The solid line is the seawater evaporation-dilution trajectory (Carpenter, 1978). The empty circle represents the extent of seawater evaporation. Sample IDs are shown for 5 points, which lie above the seawater trajectory. (b) The Cl/Br versus Na/Br for the same formation waters. The same 5 points in panel a are labeled here. The trajectory of seawater evaporation beyond halite saturation is shown (dashed line), as is the path of halite dissolution. The solid line is the relation for incongruent halite dissolution in pure water (Stueber and Walter, 1994).

resulted from seawater evaporation to various points beyond halite saturation. This reduces the Cl/Br ratios in the waters because halite preferentially removes Cl relative to Br. At different locations, the degrees of seawater evaporation and halite precipitation are different, explaining the scatter seen in the data.

Importantly, about five of the water samples lie appreciably above the seawater trajectory (those labeled with well IDs). These represent subsequent mixing of the halite-saturated residual saline waters with fresh meteoric water. Because of this dilution, the residual waters became undersaturated with halite, thus dissolving Br-poor halite and increasing

the Cl/Br ratio of the waters. The Cl/Br versus Na/Br crossplot further strengthens this explanation (Figure 10b). Formation waters that have evolved from seawater through halite precipitation or dissolution should define a Cl/Br-Na/Br trajectory that originates at the seawater and has a slope consistent with equimolar decreases or increases in Cl and Na (Walter et al., 1990). The previous data with Cl/Br higher than seawater (5 labeled in Figure 10a) are also labeled in this ratio plot. With the exception of well ID 8, all others are clustered around the halite dissolution line. The rest of the data (with Cl/Br below the seawater trajectory in Figure 10a) lie close to the halite precipitation line.

Finally, although the timing of such freshwater invasion cannot be determined based on the geochemistry data alone, a significant unconformity exists between the Cretaceous (i.e., Mesaverde Group) and the Tertiary formations (Szpakiewicz and Collins, 1985). This paleohydrologic condition was favorable for the meteoric invasion of the Cretaceous marine rocks, resulting in the mixing of fresh waters with the marine connate water. This is qualitatively consistent with the warmer temperature inferred for the recharge waters. Because the Tertiary deposition was nonmarine and most of the waters in the sediments during this deposition were likely continental and meteoric, the marine signature seen in the isotope analysis is likely pre-Tertiary. A few of these waters came from the nonmarine Wasatch wells, hinting a possibility of deeper marine water upwelling (note that such waters had likely been modified by freshwater recharge before the Tertiary deposition). The above interpretation is restricted to waters in the southeastern basin, among the formations sampled in this study (where Na-Cl dominates the TDS, e.g., Figure 8a), because stable isotope and Br data are lacking elsewhere.

Gas Geochemistry

The natural gas in the Uinta Basin consists of methane and C_{2+} hydrocarbons (wetness by volume: 2–23%). Nitrogen and CO_2 exist in minor amounts (less than 2% by volume), with trace amounts of He, H_2, and O_2 (0.001–0.04%). In this study,

two gas dryness indexes are used (gas expressed in volume): $\log_{10}[C_1/(C_2 + C_3)]$ and C_1/C_{1-5} (C_{1-5} meaning $C_1 + C_2 + C_3 + C_4 + C_5$). The higher these indexes are, the more enriched the gas is with CH_4 relative to the higher chained hydrocarbons. Because difference in source rock, thermal maturity, migration, mixing (of gases of different origins), and secondary oxidation can all impact gas composition (Rice, 1983; Schoell, 1983; Price and Schoell, 1995), composition data alone cannot provide sufficient information on gas origin and migration. To help identify the dominant processes, both carbon and hydrogen isotopes of the gases and the geochemical makeup of associated formation waters are needed (Martini et al., 2003; McIntosh et al., 2004a, b). Based on the chemical and isotopic characteristics of the available data, the Uinta Basin gases can be divided into two groups of different source rock and potential migration pathways. Within each group, the gas shows a continuous gradation in chemical and/or isotopic compositions. The following sections will discuss these groups in detail, with respect to the composition data first, then the isotope data.

Based on the compositional data of the Uinta Basin gases, several observations are made. Gas dryness index versus CH_4 mole percent (Figure 11a) indicates that the new gases sampled in this study fall within a narrow trend defined by the preexisting gas compositional data. The composition of the Dominion Gas wells at and near the Natural Buttes (Figure 4) closely resembles the range of the new data, despite the fact that the new samples fall both within and outside this field (Figure 5). This suggests that gases in the southeastern basin may have migrated from the Natural Buttes gas field. This trend also indicates a continuous gradation in composition, from appreciably wet to fairly dry. This gradation is not related to depth (thus thermal maturity of the reservoir rocks) (Figure 12), suggesting that gas migrated from deep common source rocks into the Natural Buttes and the southeastern basin.

The associated gases of the Altamont-Bluebell and Red Wash oil fields fall outside the trend (Figure 11a). In particular, three deep wells were sampled from the Altamont-Bluebell field (Rice et al., 1992): Babcock 2-12B4 (perforation depth: 12,222 ft [3725.2 m]), Brotherson 2-11B4-1 (11,491 ft [3502.4 m]), and Chatom 1-21A4 (15,172 ft [4624.4 m]). When these three wells are compared to the other Altamont-Bluebell wells with depths less than 3 km (1.8 mi), they have the lowest dryness index and CH_4 content. Because their depths correspond to the observed interval (3–5 km [1.8–3.1 mi]) of oil production (Spencer, 1987), this explains the wetter gases present as products of thermogenesis. These three wells will be distinguished in the following analysis and their names labeled in subsequent plots. The shallower Altamont-Bluebell wells have significantly drier gases, and isotopic analysis (next) indicates biogenic components.

The CO_2 contents of the gases show more scatter although the above grouping remains coherent (Figure 11b). The shallower Altamont-Bluebell gases contain the lowest CO_2 concentrations, whereas the three deep wells have higher concentrations of both CO_2 and wetter gases indicating thermogenesis (e.g., Martini et al., 2003). The newly sampled gases again fall into the Natural Buttes composition field. The gas dryness index and the concentrations of CH_4 and CO_2 are further plotted against the perforation depth (Figure 12). The three deep Altamont-Bluebell wells producing wet gases are distinct from the others, as expected. Among the Natural Buttes gases and the new gases, no significant depth trends exist. Rice et al. (1992) noted also that gas composition does not correlate with the thermal maturity or burial depth of the reservoir rocks. This suggests gas migration from deep common source rocks and subsequent pooling in shallow reservoirs throughout the central and southeastern basin.

Isotopic characteristics of the Uinta Basin gases are evaluated within the classic compositional field from Schoell (1983) (Figure 13). In general, gas sourced from the oxygen-rich type III kerogen exhibits less variation in CH_4 $\delta^{13}C$ and is chemically drier than those sourced from the hydrogen-rich (types I and II) kerogen. At similar thermal maturity, gas from type III kerogen is also heavier in CH_4 $\delta^{13}C$ than those of types I and II kerogen. In the Uinta Basin, the Altamont-Bluebell wells

Figure 11. Composition crossplots of the Uinta Basin gases: (a) gas dryness index versus CH_4 mole percent; (b) CO_2 content versus CH_4 mole percent. Three deep wells from the Altamont-Bluebell are distinguished; all other Altamont-Bluebell wells have a sampling depth less than 3 km (1.8 mi) (Rice et al., 1992).
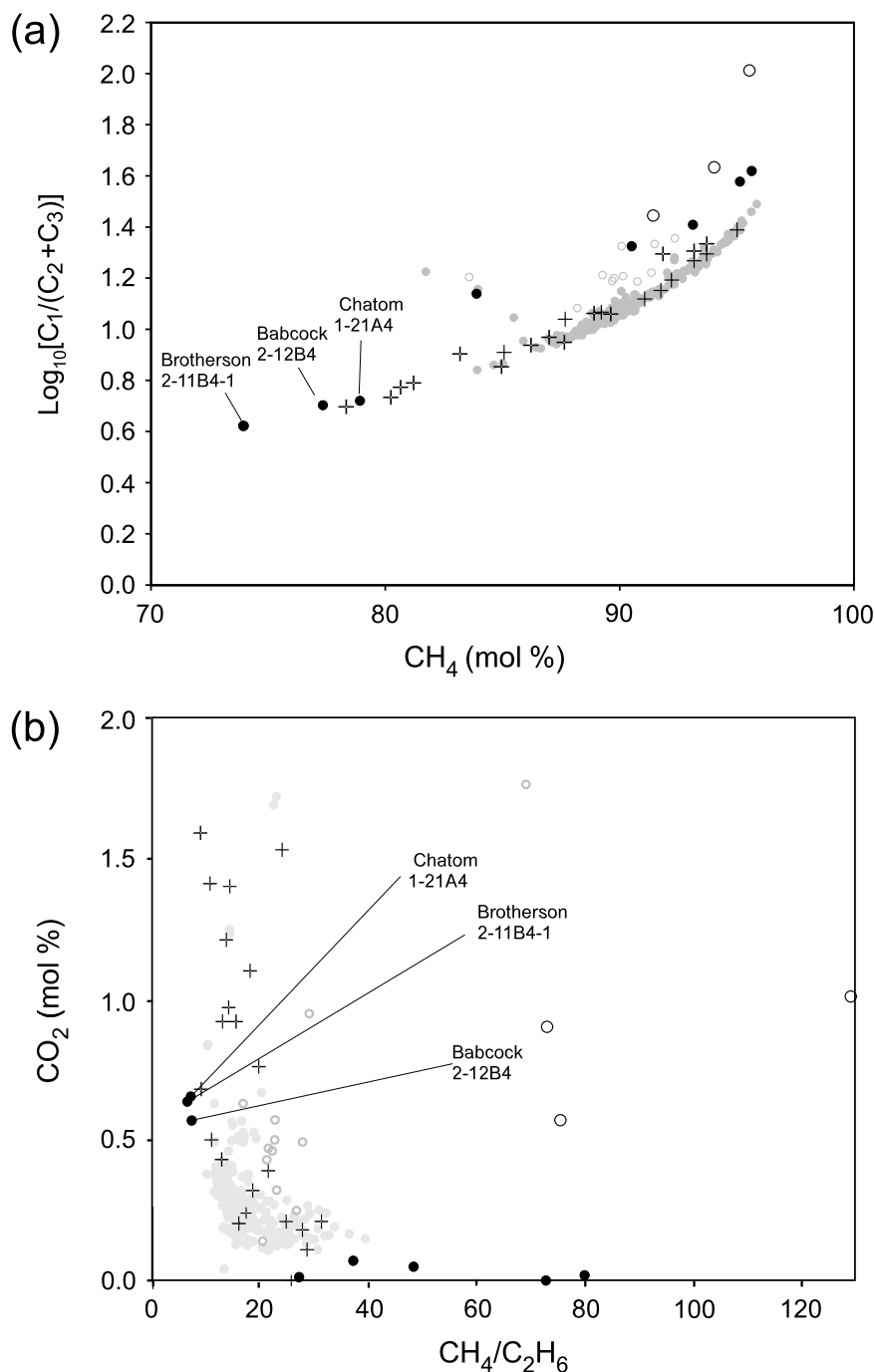
have the expected split between thermogenic (three deep wells producing associated gases falling within the thermogenic field of type I and II kerogen) and nonthermogenic and possibly mixed biogenic gases (shallow wells producing from the Green River Formation falling within the immature, mixed gas

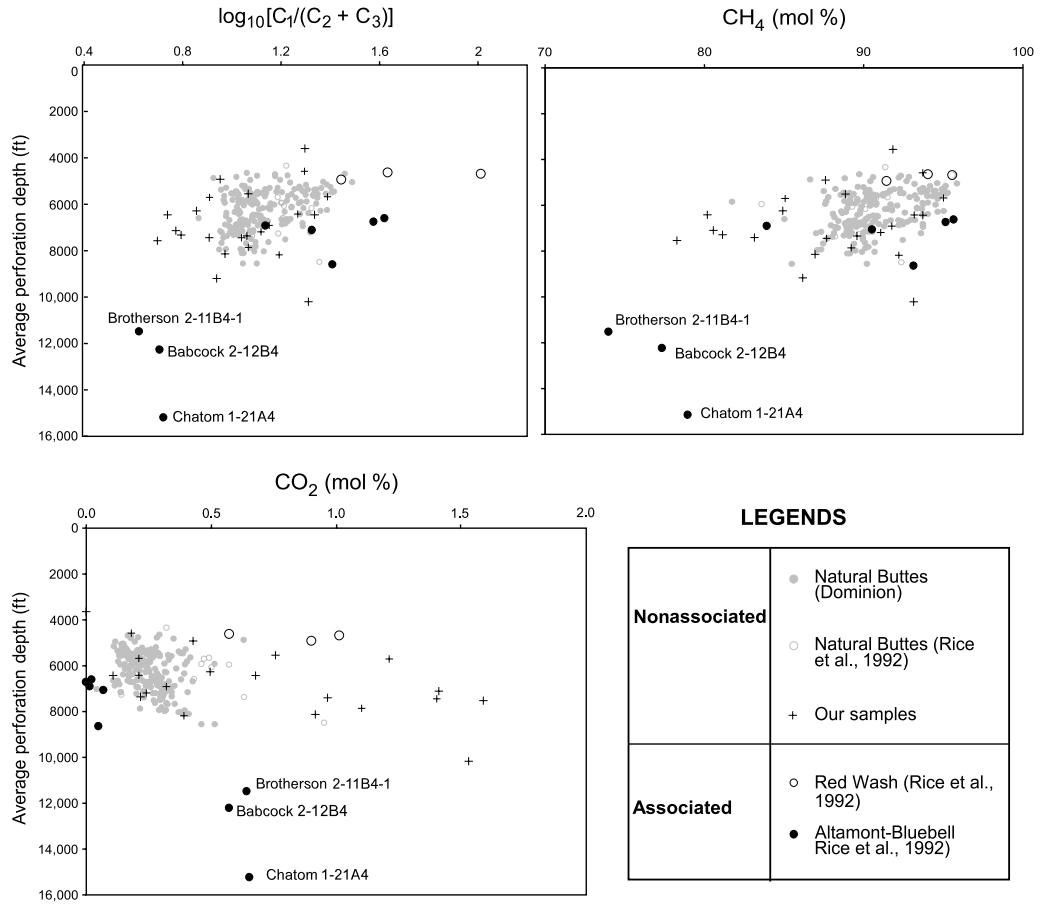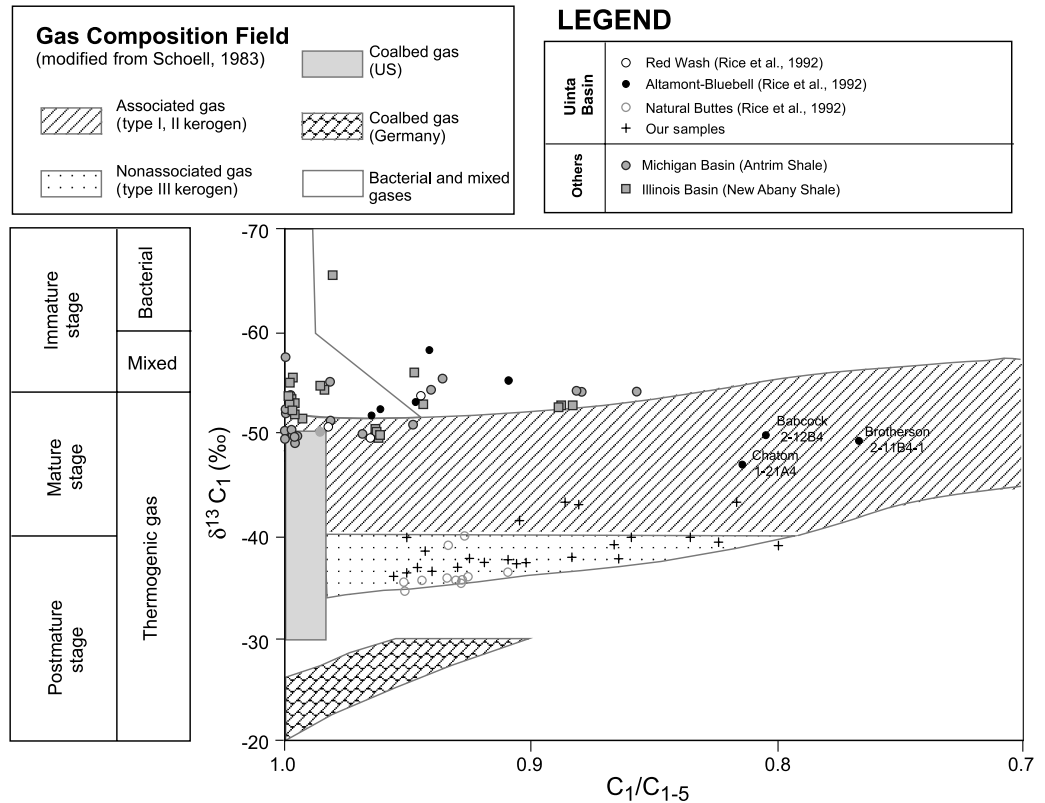**Figure 12.** Gas composition data (Dryness index, CH_4, CO_2) versus perforation depth.

Figure 13. Gas dryness index versus methane $\delta^{13}C$ of the Uinta Basin, superimposed onto a modified compositional field (Schoell, 1983). Biogenic gases from the Michigan and Illinois basins are plotted for comparison.

field). This is consistent with the fact that the Green River shale contains type I kerogen (Fouch et al., 1992; Ruble et al., 2001). The shallower, biogenic signature can be supported by the fact that the Green River shale is immature to marginally mature in much of the basin (Schamel, 2005). At the Altamont-Bluebell field, the R_o of the Green River Formation is above the oil window when the depth is less than 9000 ft (2750 m) (Figure 2). These shallower Altamont-Bluebell wells fall into this range (Figure 12). Furthermore, salinity mapping (shown below) identifies freshwater invasion into the northern basin; the shallow, immature, commonly fractured Green River shales could provide a suitable substrate for microbial methanogenesis.

Most of the Natural Buttes gases (Rice et al., 1992) and the new gas samples fall within the nonassociated thermogenic gas with the source rock type identified as type III kerogen (Figure 13). This is consistent with the fact that, in the central to northern basin, the Mesaverde Group is deeply buried, thermally mature, and contains type III kerogen (Anders et al., 1992; Nuccio et al., 1992; USGS, 2002; Johnson and Roberts, 2006). The above division in the composition or isotope field is repeated when CH_4 $\delta^{13}C$ is plotted against CH_4 δD and depth (not shown). The separation between the associated and nonassociated gases is again clear. Among the two Altamont-Bluebell subgroups, $\delta^{13}C$ is slightly more positive for the deeper wells, corresponding to enrichment in thermogenic gases. For the nonassociated gases, similar to the composition data, methane $\delta^{13}C$ does not vary with depth.

Overall, for the nonassociated gases, the lack of depth-dependence in both gas composition and stable isotopes suggests that such gases may have originated from common source rocks at depth. The Mesaverde Group contains type III kerogen in coals and carbonaceous shales, and at the Natural Buttes, it is marginally mature for gas generation. It is immature in the southeastern basin because of the shallower burial depth (USGS, 2002). The overlying Wasatch Formation in the central to southeastern basin is mostly immature for gas generation. An overall picture thus emerges as that of a common thermogenic source rock in the deeply buried Mesaverde, possibly underlying and to the north of the Natural Buttes (where Mesaverde maturity reaches the maximum, USGS, 2002). This is consistent with the projections of thermal maturity, fluid pressure, and geochemical indicators, which combine to suggest the presence of a regional-scale overpressured gas deposit in the deeply buried Mesaverde strata in the northern basin (Spencer, 1987; Fouch et al., 1992). At the Natural Buttes, the extensive and prolific gas fields may have formed because of the extensive fracture system near the basin center, which could have provided the migration pathways to these reservoirs (Figure 4). In the southeastern basin, this deep gas has further migrated into the shallower, thermally immature reservoirs of the Mesaverde Group and Wasatch Formation, explaining the similar genetic makeup of the gases with those of the Natural Buttes. This inferred gas migration is from the basin center toward the southeast, opposite of the regional hydraulic gradient (Holmes, 1985; Wanty et al., 1991; Robson and Banta, 1995), and updip along the formations toward the basin margin. Such a pathway is thus consistent with a thermogenic origin. This pathway suggests that deep-gas genesis and expulsion were forceful enough to displace formation waters instead of in-situ gas biogenesis, which is driven by freshwater recharge. This gas migration is likely in separate phase, as multiphase flow analysis has demonstrated that although groundwater flows downdip in a regional aquifer, depending on the formation dip, the less dense gas phase can migrate updip driven by its buoyancy (Ingebritsen et al., 2006, their section 7.2.3, Secondary Migration).

To summarize, the division between the associated and nonassociated gases in the Uinta Basin can be attributed to the differences in source rock type, burial depth, and whether biogenic versus thermogenic processes dominated in either case, given the presence or absence of significant freshwater drive. The generation and migration mechanism of the nonassociated gases in the central to southeastern basin appear very different from those of the northern basin where a biogenic signature is observed at depths less than 9000 ft (2750 m), indicating the influence of freshwater recharge on gas genesis within the immature Green
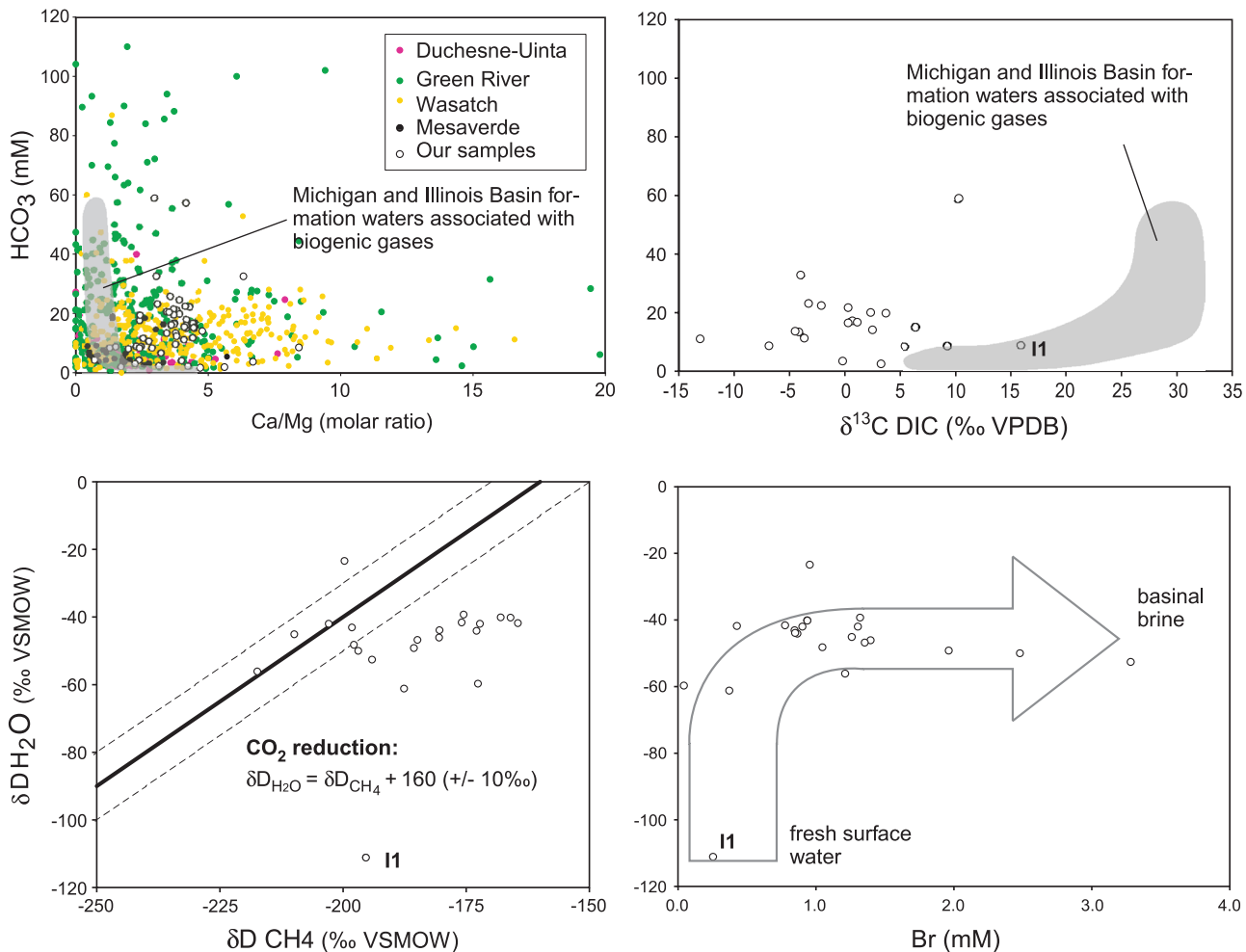
Figure 14. Crossplots exploring water-gas genetic links. Note that the preexisting water chemistry database does not contain isotope information and Br concentrations. The gray envelopes encompass the relevant ranges for the Michigan and Illinois basins' biogenic gases and coproduced formation waters. DIC = dissolved inorganic carbon; SMOW = standard mean ocean water; VPDB = Vienna Peedee belemnite.

River shales. Because the organic facies of the Green River Formation and the Mesaverde Group exist throughout the basin, besides the burial depth, this overall division reflects the difference in strength of the regional hydrodynamics. Compared to the vigorous northern flow system, groundwater movement in the southeastern basin is more sluggish because of the reduced topography and precipitation rate (Topographic Map Series of the United States, NJ 12-3; USWP, 1999).

Gas and Water Isotopes

The biogenic versus thermogenic origin of gases can also be elucidated by the systematics of major

elements and stable isotopes of the coupled water and gas samples. In particular, the water chemistry is commonly affected significantly by methanogenesis (McIntosh et al., 2004a, b): (1) high HCO_3 concentration (in the range of 10–70 mM), typically accompanied by lower Ca/Mg mole ratios (less than 1.5), caused by low-Mg carbonate precipitation; (2) positive $\delta^{13}C_{DIC}$ (greater than 20‰), and positive gas $\delta^{13}C_{CO_2}$ (greater than 10‰); (3) covariance of δD of CH_4 and coproduced water. For samples analyzed in this study, the relevant indicators are plotted in two sets of crossplots (Figure 14, top and bottom rows). In the top row, the HCO_3 concentration is plotted against Ca/Mg and $\delta^{13}C_{DIC}$, respectively. For comparison, those of the immature

shale waters associated with gas biogenesis in the Michigan and Illinois basins are shown (Martini et al., 1998; McIntosh et al., 2004a, b). In the bottom row, the isotope equilibrium function between δD_{CH_4} and δD_{H_2O} for microbial fractionation of methane and water via CO_2 reduction is superimposed as a solid line bracketed by ±10‰ error bars, following Schoell (1980). Because deep basinal brines typically have high Br concentrations and high δD_{H_2O} values, the δ_{DH_2O} versus Br concentration is also plotted.

The elemental and stable isotope cross plots of the coupled water and gas samples from the central to the southeastern Uinta Basin do not exhibit significant biogenic signatures. Although HCO_3 concentrations in such waters are comparable to those in the waters of the Michigan and Illinois basins, their $\delta^{13}C_{DIC}$ is significantly more negative. The δD versus Br relations suggest that the Uinta Basin samples originated as basinal saline fluid instead of fresh meteoric water (I1 is contaminated with surface water, Figure 9), again conditions unfavorable for biogenesis. Most of the Uinta Basin data also deviate from the equilibrium relations predicted for biogenic CO_2 reduction. The $\delta^{13}C_{CO_2}$ of the sampled gases is negative (Table 5; see AAPG Datashare 32), consistent with the other parameters and indicating thermogenesis. However, as noted earlier for the group of high-HCO_3-low-SO_4 Green River waters, a significant fraction of such waters falls within the biogenic envelope of the immature shale waters in the Michigan and Illinois basins. Thus, future sampling should focus on the shallow Green River shales in the central to northern Uinta Basin to identify their $\delta^{13}C_{DIC}$ range as well as the other biogenic indicators. Currently, however, oil production tends to be the focus in this part of the basin and the biogenic gas plays remain mostly underdeveloped (Schamel, 2005).

## Three-Dimensional Relations for Formation Fluids

To further understand fluid migration in the Uinta Basin and to strengthen the previous interpretations of migration pathways based on chemical relations, data from the preexisting records and the new samples are combined to form the basis for a three-dimensional (3-D) analysis of basin scale trends in TDS, major elements, and gas composition. (Unfortunately, minor element and stable isotope data are too sparse to permit interpolations at this large scale.) To accomplish this, a hydrostratigraphic model of the basin was built with the gridding toolbox LaGriT (Los Alamos National Laboratory, 2009), using topographic and isopach maps of the major formations (Willett and Chapman, 1987; Topographic Map Series of the United States NJ 12-3; Glover, 1996; Glover et al., 1998) (Figure 15). Because too little well data from the Mancos Shale exist to allow an adequate characterization of formation water geochemistry, the Mancos Shale is not included in the model.

To generate a realistic model, surface elevation of each formation contact is interpolated with a geostatistical algorithm, i.e., the elevation of data points on the contact is considered a spatially correlated random variable. Because all surfaces are trended, a linear, isotropic variogram model is fitted to a global omnidirectional experimental variogram of the elevation. This variogram model is then used by ordinary kriging to generate an interpolated surface, which represents a smoothed formation contact (thus, locally abrupt changes caused by fault displacements cannot be represented). This process is repeated for all major formations. The resulting surfaces are then used by LaGriT to generate a hydrostratigraphic model of a hexahedral grid with 236,277 nodes and 210,058 elements. For the deeply buried strata bordering the Uinta Mountains, local grid refinement is employed to capture the continuity of the steep stratigraphic incline and relatively thin beds. Compared to the existing basin geology and structure data, this grid has captured the overall extent, shape, and thickness of the major formations. Compared to the spatial coverage of the geochemical database, the hydrostratigraphic model is extended eastward to incorporate the Douglas Creek arch, where the coal-bearing Mesaverde Group forms extensive outcrops (Freethey and Cordy, 1991). This allows for the incorporation of future data, which will be collected from this region.
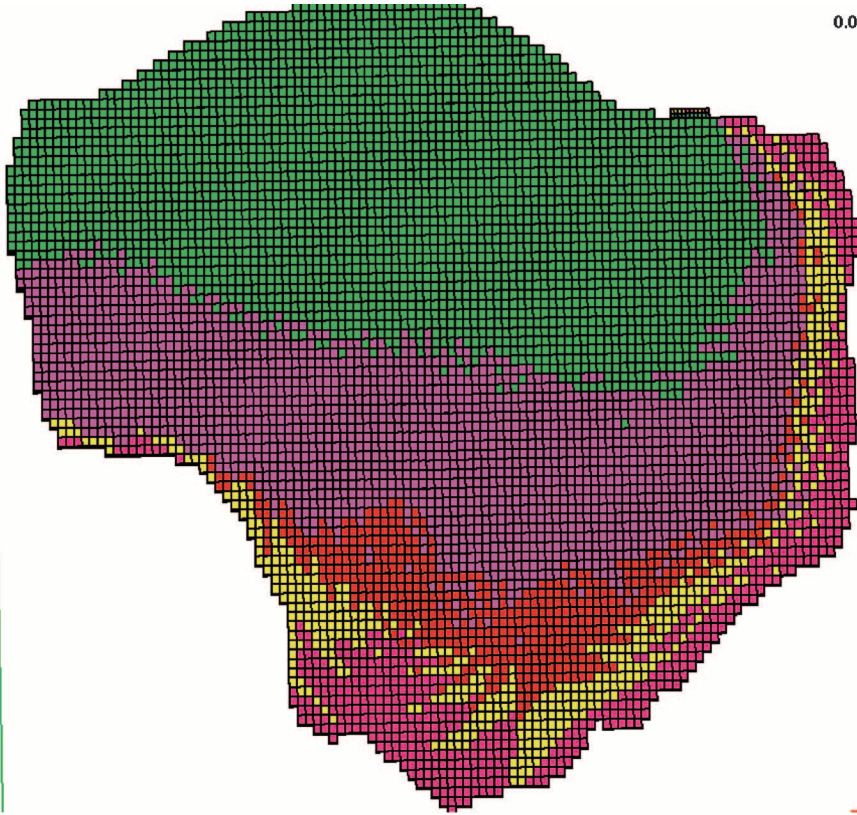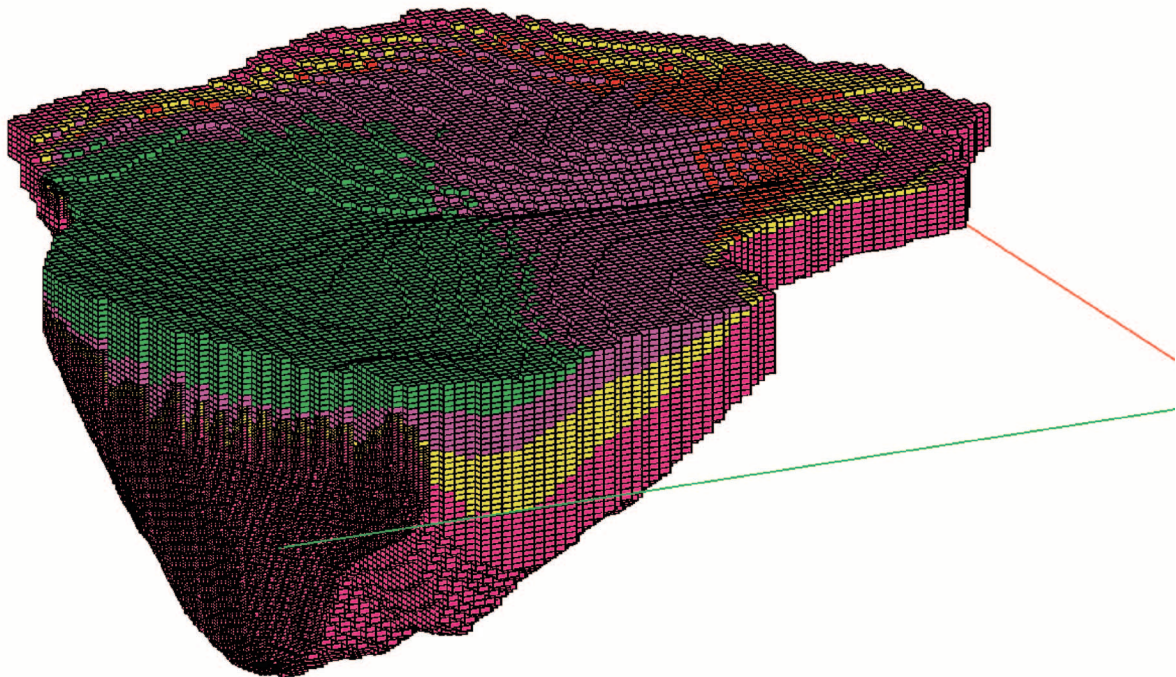
Figure 15. A model of the Uinta Basin with five major hydrostratigraphies (from top to bottom): Duchesne-Uinta aquifer (green), Parachute Creek confining unit of the Green River Formation (purple), Douglas Creek-Renegade aquifer of the Green River Formation (red), Wasatch-Green River confining unit (yellow), and Mesaverde Group (dark red). These divisions are based on Glover et al. (1998). The plots employ a 10× vertical exaggeration.
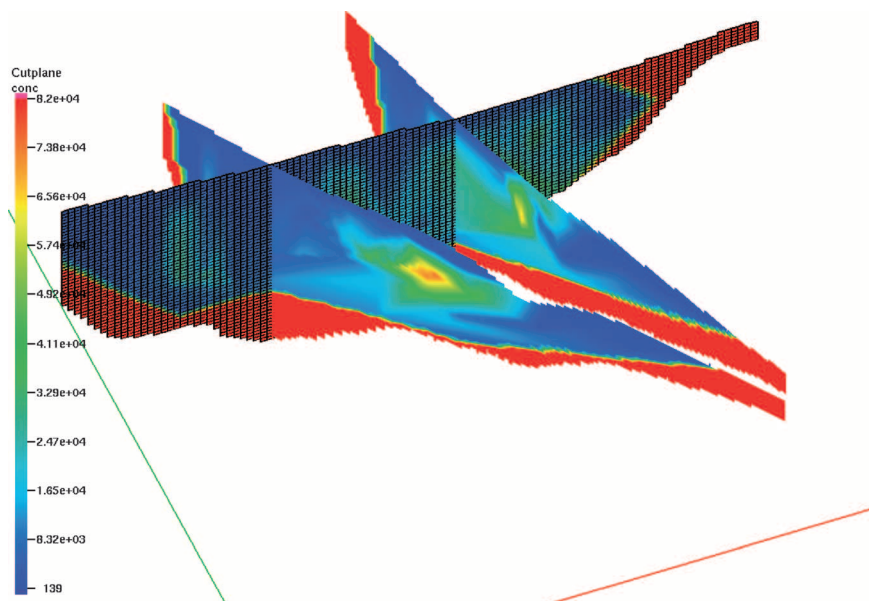
Figure 16. Uinta Basin formation water TDS (mg/L) projected onto several basin-scale cross sections. Regions with no chemistry data are given the highest value (red) and should be ignored. The thickest part of the vertical transect points to the north.

The model clearly reveals the significant asymmetry in basin stratigraphy. Geographically, the deposit of the Duchesne-Uinta aquifer is seen throughout the northern basin, whereas the extensive outcrops in the southern basin consist of the members of the Green River Formation, the Wasatch Formation, and the Mesaverde Group. Significant thickening of the Green River and Wasatch formations occurs toward the north where hydrocarbon generation in the deeply buried lower Green River Formation has created the observed overpressure at depth. Importantly, the dramatic northward increase in the burial depth of the Mesaverde Group (basal unit of the model) corresponds to increasing thermal maturity of the organic matters in this formation (USGS, 2002). The deeply buried part of the Mesaverde Group is likely the source rock for many of the type-III-kerogen-sourced gas deposits in the basin.

The combined water geochemistry database contains 897 samples for which the TDS data are projected onto several cross sections (Figure 16). The regional topographic lows along these transects correspond to the depression surrounding the Green River Valley. Each sample location is translated to an [x,y,z] coordinate point consistent with the model coordinate (x-y origin is at the corner of southwestern basin and z represents the elevation above sea level). Because the model

domain is slightly larger than the available data coverage, regions of the model without data are given the maximum TDS + 1.0, thus such regions (shown in red) should be ignored. Although not shown, the mapping of Na and Cl concentrations along the same transects presents nearly identical patterns as the TDS variation (also see Figure 7, where Na-Cl type dominates the high-TDS waters). Clearly, regional southward migration and upwelling of Na-Cl type waters from 2- to 3-km (1.2- to 1.8-mi) depth are responsible for the elevated salinity observed in the shallow aquifers and springs along the Green River Valley. In the northern basin, despite the fact that the Wasatch Formation is more deeply buried than its southern counterpart, a freshwater lens (up to 6 km deep) is evident, indicating that meteoric water has invaded into this formation. This confirms the earlier observed low Wasatch salinity in the depth plot (Figure 6), as well as in comparison to the new waters sampled from the equivalent formations in the southeastern basin (Figure 8a).

Thin layers of Paleozoic and Mesozoic rocks were thrust upward along the south flank fault between the basin and the Uinta Mountains (Fouch, 1975; Pitman et al., 1982). These units are generally permeable formations, providing a pathway for downward moving flows (Zhang et al., 2005). The freshwater lens is also regionally significant,

overlapping members of the Green River Formation at shallower depths, providing suitable geochemical environment for microbial methanogenesis. This encroachment of meteoric waters was locally confirmed by the isotopic composition of carbonate cements in the Green River Formation (Pitman et al., 1982), taken from borehole samples down to 6000 ft (1828.8 m) in the Pariette Bench field (part of the Greater Monument Butte, Figure 4). Pitman et al. (1982, p. 1581) concluded that the "authigenic carbonate formed at low temperatures in the presence of meteoric waters by a process of solution-precipitation." In the northern basin, however, because of the lack of minor elements and stable isotope water chemistry data, the timing of such freshwater recharge cannot be determined.

The Green River Valley constitutes a regional topographical low (Figure 15), contributing to a high hydraulic gradient, which directs groundwater flow toward the river. This high hydraulic gradient, combined with locally elevated permeability (e.g., various fractured zones in the central basin as mapped by Fouch et al. [1992] and Nuccio et al. [1992]), allows enhanced fluid flow along these pathways. This is consistent with the TDS mapping, which indicates that saline waters are converging toward the Green River (Figure 16). This is also consistent with the inferred flow directions based on the potentiometric surfaces (Figure 3), and the observed regional-scale thermal anomalies (Willett and Chapman, 1989). The subsurface temperature gradient is depressed beneath the northern margin of the basin and enhanced beneath the central basin discharge areas (Willett and Chapman, 1989).

Because the flow rates of hydrocarbons are also determined by gradient and permeability, these preferential pathways for groundwaters will likely provide pathways for hydrocarbons. Indeed, oil will migrate in the direction of groundwater flow, but with an upward drift caused by its lower densities (Ingebritsen et al., 2006). Studies on oil composition and thermal maturity at the Pariette Bench field (down gradient from Altamont-Bluebell) indeed suggest oil migration from the deeply buried Green River source rocks farther to the north (Pitman et al., 1982). However, the overpressure caused by oil generation at the depth of the northern basin is likely important in driving this migration. Moreover, gas migration (as a separate phase) can occur in the same direction or opposite of groundwater flow, depending on the formation dip and fluid density contrast. In the northern basin (where salinity mapping indicates groundwater converging downdip toward the central basin), gas migration will likely also move downdip. However, because of the lack of gas data in this region and the fact that existing water chemistry data did not report the dissolved gas content, the exact form of gas migration, dissolved in water or as a separate phase, cannot be determined. To definitely answer this question, it will be relevant in the future to sample both waters and gases along these pathways.

Data from 240 gas samples (combining the Dominion Gas data and the new samples) are used for mapping the gas composition at the regional scale from the Natural Buttes toward the southeastern basin (Figure 17, top panel). The gas data from the northern basin are too sparse with incomplete location information to allow meaningful interpolations there. Compared to the water geochemistry data (Figure 5), the gas data are much more limited in spatial and depth coverage (Dominion Gas shown in Figure 4 and new samples shown in Figure 5). Because most gas data are from the Wasatch Formation and Mesaverde Group (the bottom two units of the model), the mapping shows this limitation, as no data exist for the shallower formations. However, an extensive enrichment of CH_4 (in mole percent) near the Natural Buttes gas field is evident, occurring at depths approximately 5000 to 6000 ft (1524 to 1828.8 m). The CH_4 contents also decrease as the distance from Natural Buttes increases. This trend suggests a reverse chromatographic effect: as gas migrates, lighter compound such as methane is continually removed because of its higher aqueous solubility compared to gases of higher carbon numbers (McAuliffe, 1978). This is consistent with the observed gas compositional gradation (Figure 11a), the interpretation of separate phase flow (discussed previously), and the proposed migration direction of
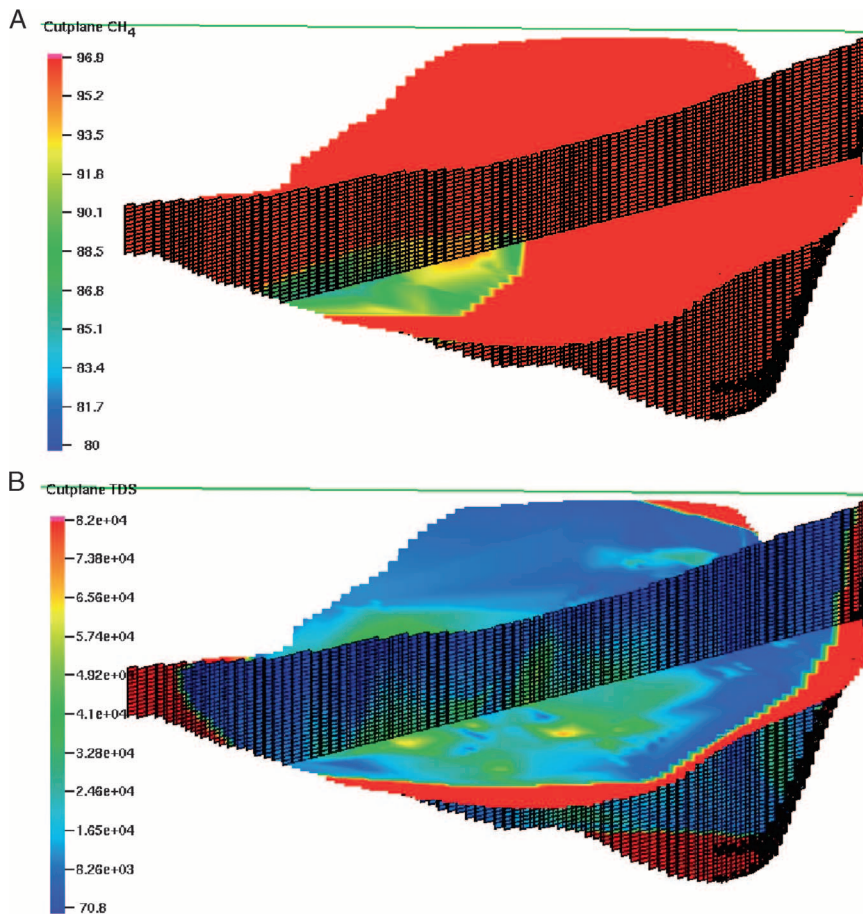
Figure 17. Methane concentrations (in mole percent) (top) and formation water TDS (mg/L) (bottom) projected onto the same two cross sections. The thickest part of the vertical transect points to the north. TDS = total dissolved solids.

the thermogenic gases from the basin center toward the southeast. Interestingly, near the basin center, the upwelling of saline waters toward the Green River is again apparent (Figure 17, bottom panel) (recall that the combined water chemistry database is much more extensive in spatial coverage), indicating preferential flow paths for the formation fluids migrating into the shallower strata. Such flow direction, as visualized by the TDS anomalies, indicates the possibility that gas deposits may be found in localized traps along these pathways, above the average depths of the Natural Buttes wells. Indeed, in the central basin, the Green River Formation forms multiple reservoirs and caprock units (see the facies mapped beneath the Natural Buttes, Figure 2). However, this concept requires more detailed and localized structural and stratigraphic mapping to evaluate the existence of such traps.

Finally, note that using geochemical data to understand subsurface flow dynamics has limita-tions. (1) The geochemistry pattern reflects a snapshot of the more recent conditions. To understand the effects of fluid migration and solute transport during the geological time, numerical modeling is needed. (2) The interpretation based on the geochemistry data is limited to scales larger than that defined by the sampling density. Small-scale effects beneath the sampling grid (e.g., caused by the local-scale flow dynamics and heterogeneity) will not be revealed. In fact, research on basin-scale flow dynamics suggests the existence of local variability in flow and reaction, superimposed onto the regional-scale trend (Ingebritsen et al., 2006). Thus, the complex flow dynamics in the Uinta Basin, as discussed in the Introduction, may only be partially revealed. However, the overall regional trend as inferred from the chemistry data is not inconsistent with the hydraulic data (Figure 3). Our TDS mapping is also consistent with maps of geochemical water types projected along two basin-scale cross sections (Szpakiewicz and Collins, 1985). Their

maps also show the upwelling of Na-Cl–type waters toward the central basin discharge areas. In the northern basin, the southward migration of saline waters (and possibly oil) can be driven by both the topographic gradient of the Uinta Mountains and the deep fluid expulsion from the overpressured lower Green River Formation. Future work will use numerical modeling to quantify the relative importance of each driving force.

SUMMARY AND CONCLUSIONS

The geochemistry of formation waters and hydrocarbon gases in the Uinta Basin, Utah, is evaluated at the regional scale based on fluid sampling and compilation of existing records. The formation water chemistry in the deeply buried basin strata is dominated by Na-Cl type. In the southeastern basin where minor elements and stable isotopes were analyzed, the origin of such Na-Cl waters is interpreted to be a mix of ancient evaporatively concentrated seawater with meteoric water recharged in the geological past, which has also experienced water-rock interactions. The dominant water-rock reactions thus include (1) NaCl precipitation from ancient seawater and subsequent dissolution when fresh meteoric water invaded (this gave rise to the overriding Na-Cl signature in the deep flow system where halite dissolution has the greatest effects on water chemistry); (2) dissolution of evaporites, particularly sodium carbonates and anhydrite, contributing additional Na, Mg, HCO_3, and SO_4 to the deep waters; and (3) in the shallower system near the recharge areas (depth <2000 ft [609.6 m]), dissolution of feldspar and carbonate, clay mineral formation, and ion exchange, resulting in the typical recharge-type low-TDS Na-Ca-Mg-HCO_3-Cl waters. These reactions are only significant in a local sense; their signature is overwhelmed when viewed at the regional scale, where halite dissolution contributes significantly to the total TDS in the deeper flow system (Figure 7).

In addition to water-rock reactions, 3-D mapping of the water geochemistry at the basin scale reveals the importance of regional-scale flow dynamics and solute transport. (1) In the northern Uinta Basin bordering the Uinta Mountains, significant flushing of the deep basinal saline waters at up to 6-km (3.7-mi) depth by meteoric water has occurred. (2) In the central basin groundwater discharge areas (the Green River Valley), regional upwelling of saline waters from 2- to 3-km (1.2- to 1.8-mi) depth is occurring. Both observations have significant implications for studies of natural versus anthropogenic sources of salinity in shallow aquifers and rivers in this basin. Based on the available data, the overall geochemical makeup of the formation waters in the Uinta Basin is thus controlled by both the lithology of the geological formations and regional flow dynamics.

Based on the available data on water and hydrocarbon gas geochemistry, the Uinta Basin gases can be divided into two groups. (1) Associated gases of the Green River Formation (Altamont-Bluebell and Redwash oil fields) are characterized by methane $\delta^{13}C$ of 60 to −45‰, methane δD of −280 to −225‰, and a gas dryness index (C_1/C_{1-5}) ranging from 0.76 to 0.98. These gases are interpreted to be thermogenic (reservoir depth >9000 ft [2750 m]) and mixed thermogenic and biogenic (depth <9000 ft [2750 m]); the source rock type is type I kerogen of the Green River Formation. (2) Nonassociated gases of the Wasatch Formation and Mesaverde Group in the Natural Buttes gas field and the southeastern basin are characterized by methane $\delta^{13}C$ of −42 to −34‰, methane δD of −220 to −165‰, CO_2 $\delta^{13}C$ of −1.1 to −12.5‰, and a gas dryness index ranging from 0.80 to 0.96. The $\delta^{13}C$ of DIC in the coproduced waters ranges from −6.8 to 15.9‰. These gases are interpreted to be thermogenic, originating from the type III kerogen of the deeply buried, thermally mature Mesaverde Group in the central to northern basin. Moreover, gas migrates from the basin center toward the southeast, opposite of the regional hydraulic gradient, giving credence to the hypothesis of formation fluid expulsion caused by gas generation (Cathles and Adams, 2005). Compared to the vigorous northern flow system, groundwater in the southeastern basin is more sluggish, likely a result of the reduced topography and low recharge rate.

In the Uinta Basin, the various processes summarized above comprise a complex and coupled

system of regional-scale fluid flow, solute transport, and hydrocarbon generation and migration. To provide insights into the dominant geochemical and fluid-flow processes, integrated gas and water compositions along with relevant stable isotope data are required. The contribution of this study is thus the interpretation of basin-scale water and gas geochemistry within a hydrogeological framework. This interpretation is enhanced by innovative geological model building combining regional structure and stratigraphic data with geostatistics. Our work suggests that studies of hydrogeochemistry should take into consideration both the geochemistry of the formations through which fluids migrate as well as the external or internal forcings that drive flow and cause long-distance migration. In basins surrounded by uplifted mountain ranges, enhanced recharge along the mountain fronts may significantly impact groundwater flows at depth. However, fluid overpressure caused by hydrocarbon generation in the deeply buried organic-rich strata will introduce additional complexities to the interpretation of the deeper flow system.

To facilitate a quantitative understanding of the complex interplays between groundwater flow and solute transport, future work will consider a mass balance calculation along selected recharge-to-discharge flow paths (Parkhurst et al., 1982; McIntosh et al., 2004a, b). Such calculations will identify important sources and sinks for salinity (and more generally, formation fluid composition) and its spatial relationship with the lithologies along the flow paths (which can be mapped using borehole data and geostatistics). In turn, this information will be used to constrain a coupled numerical model of variable-density groundwater flow and reactive solute transport in the basin. The geochemical database compiled in this study will provide the critical ground-truth information to help calibrate the numerical models and verify the simulation predictions. To evaluate fluid-flow processes over geological times, this model can be deformed to create a basin evolution model, which can be used to quantify the relative importance of various fluid driving mechanisms (McPherson and Bredehoeft, 2001). The Uinta Basin is not unique in its geological complexity, and this integrated approach can potentially be developed into a new methodology for regional-scale hydrogeological characterization. The hydrogeochemical and hydrocarbon framework developed in this study will have ramifications for the studies of other intermontane basins in the Rocky Mountain region, which exhibit similar age, geology, and fluid-flow characteristics as the Uinta Basin.

REFERENCES CITED

Anders, D. E., J. G. Palacas, and R. C. Johnson, 1992, Thermal maturity of rocks and hydrocarbon deposits, Uinta Basin, Utah, *in* T. D. Fouch, V. F. Nuccio, and T. C. Chidsey Jr., eds., Hydrocarbon and mineral resources of the Uinta Basin, Utah and Colorado: Utah Geological Survey, Utah Geological Association Guidebook, p. 20.

Bredehoeft, J. D., J. B. Wesley, and T. D. Fouch, 1994, Simulation of the origin of fluid pressure, fracture generation, and the movement of fluids in the Uinta Basin, Utah: AAPG Bulletin, v. 78, no. 11, p. 1729–1747.

Burtner, R. L., 1987, Origin and evolution of Weber and Tensleep formation waters in the greater Green River and Uinta-Piceance basins, northern Rocky Mountain area, U.S.A.: Chemical Geology, v. 65, p. 255–282.

Carpenter, A. B., 1978, Origin and chemical evolution of brines in sedimentary basins: Oklahoma Geological Survey Circular, v. 79, p. 60–77.

Cathles, L. M., and J. J. Adams, 2005, Fluid flow and petroleum and mineral resources in the upper (<20 km) continental crust: Economic Geology, 100th Anniversary Volume, p. 77–110.

Chidsey Jr., T. C., S. Wakefield, B. G. Hill, and M. Hebertson, 2005, Oil and gas fields map of Utah: Utah Geological Survey Map 203 DM, scale 1:700,000, 1 sheet.

Clark, I., and P. Fritz, 1997, Environmental isotopes in hydrogeology: Boca Raton, Lewis Publishers, 352 p.

Craig, H., 1961, Isotopic variations in meteoric waters: Science, v. 133, p. 1702–1703.

Duffy, C. J., J. J. Jurinak, S. Sangani, and A. Azimi, 1985, Identification and modeling of the impact of marine shale bedrock on groundwater and stream salinity, upper Colorado River Basin: Utah Water Research Laboratory, Hydraulics and Hydrology Series, UWRL/H-85/01, Logan, Utah, 104 p.

Dyni, J. R., 1996, Sodium carbonate resources of the Green River Formation: U.S. Geological Survey Open-File Report, p. 96–729.

Fouch, T. D., 1975, Lithofacies and related hydrocarbon accumulations in Tertiary strata of the western and central Uinta Basin, Utah: Rocky Mountain Associated of Geologists 1975 Symposium, p. 163–173.

Fouch, T. D., V. F. Nuccio, J. C. Osmond, L. MacMillan, W. B. Cashion, and C. J. Wandrey, 1992, Oil and gas in uppermost Cretaceous and Tertiary rock, Uinta Basin,

Utah, *in* T. D. Fouch, V. F. Nuccio, and T. C. Chidsey Jr., eds., Hydrocarbon and mineral resources of the Uinta Basin, Utah and Colorado: Utah Geological Survey, Utah Geological Association Guidebook, no. 20, p. 9–48.

Fouch, T. D., V. F. Nuccio, D. E. Anders, D. D. Rice, J. K. Pitman, and R. F. Mast, 1994, Green River (!) petroleum system, Uinta Basin, Utah, U.S.A., *in* L. B. Magoon and W. G. Doe, eds., The petroleum system—From source to trap: AAPG Memoir 60, p. 399–421.

Freethey, G. W., and G. E. Cordy, 1991, Geohydrology of Mesozoic rocks in the upper Colorado River Basin in Arizona, Colorado, New Mexico, Utah and Wyoming, excluding the San Juan Basin: U.S. Geological Survey Professional Paper 1411-C, 118 p.

Freethey, G. W., B. A. Kimball, D. E. Wilberg, and J. W. Hood, 1988, General hydrogeology of the aquifers of Mesozoic age, upper Colorado River Basin—excluding the San Juan Basin—Colorado, Utah, Wyoming, and Arizona: U.S. Geological Survey Hydrologic Investigations Atlas HA-698, scale 1:2,500,000 and 1:5,000,000, 2 sheets.

Glover, K. C., 1996, Ground-water flow in the Duchesne River-Uinta aquifer, Uinta Basin, Utah and Colorado: U.S. Geological Survey Water Resources Investigation Report 92-4161, 24 p.

Glover, K. C., D. L. Naftz, and L. J. Martin, 1998, Geohydrology of Tertiary rocks in the upper Colorado River Basin in Colorado, Utah, and Wyoming, excluding the San Juan Basin: U.S. Geological Survey Regional Aquifer-System Analysis, USGS Water-Resources Investigations Report 96-4105, 103 p.

Gwynn, J. W., 1992, The oil well saline-water resources of the Uinta Basin, Utah: Their character and distribution, *in* T. D. Fouch, V. F. Nuccio, and T. C. Chidsey Jr. eds., Hydrocarbon and mineral resources of the Uinta Basin, Utah and Colorado: Utah Geological Survey, Utah Geological Association Guidebook, no. 20, p. 289–311.

Gwynn, J. W., 1995, Resistivities and chemical analysis of selected oil and gas field, water well, and spring waters, Utah: Utah Geological Survey Circular 87, Salt Lake City, Utah, 142 p.

Holmes, W. F., 1985, Water budget and ground-water occurrence in the Uinta Basin of Utah, *in* M. D. Picard, ed., Geology and energy resources, Uinta Basin of Utah: Salt Lake City, Utah, Utah Geological Association Publication, p. 271–275.

Holmes, W. F., and B. A. Kimball, 1985, Groundwater in the southeastern Uinta Basin, Utah and Colorado: U.S. Geological Survey Water Supply Paper, no. 2248, 47 p.

Howells, L., M. S. Longson, and G. L. Hunt, 1987, Base of moderately saline ground water in the Uinta Basin, Utah: U.S. Geological Survey Open-File Report 87-394, 59 p.

Ingebritsen S., W. Sanford, and C. Neuzil, 2006, Groundwater in geological processes, 2d ed., Cambridge University Press, Cambridge, England, p. 536.

Johnson, R. C., and R. M. Flores, 1998, Developmental geology of coalbed methane from shallow to deep in Rocky Mountain basins and in Cook Inlet-Matanuska Basin, Alaska, U.S.A. and Canada: International Journal of Coal Geology, v. 35, no. 1, p. 241–282, doi:10.1016/S0166-5162(97)00016-5.

Johnson, R. C., and S. B. Roberts, 2006, The Mesaverde total petroleum system, Uinta-Piceance Province, Utah and Colorado, *in* Petroleum systems and geologic assessment of oil and gas in the Uinta-Piceance Province, Utah and Colorado, U.S. Geological Survey Digital Data Series DDS-69-B, chapter 7, 68 p.

Law, B. E., and J. B. Curtis, 2002, Introduction to unconventional petroleum systems: AAPG Bulletin, v. 86, no. 11, p. 1851–1852.

Longman, M. W., 2003, Oil and gas fields in the Uinta Basin, Utah: The Mountain Geologist, v. 40, no. 4, p. 101–141.

Longman, M. W., and C. D. Morgan, 2008, Hydrocarbon systems and production in the Uinta Basin, Utah: Rocky Mountain Association of Geologists, Utah Geological Association Publications, 403 p.: http://www.utahgeology.org/RMAG-UGA-2008 DVD-Preface.pdf (accessed February 9, 2009).

Los Alamos National Laboratory, 2009, LaGriT (Los Alamos Grid Toolbox), operated by Los Alamos National Security, www.lagrit.lanl.gov (accessed November 20, 2006).

Lucas, P. T., and J. M. Drexler, 1975, Altamont-Bluebell: A major fractured and overpressured stratigraphic trap, Uinta Basin, Utah: Rocky Mountain Association of Geologists 1975 Symposium, p. 265–273.

MacMillan, L., 1997, The greater Natural Buttes producing area, southeastern Uinta Basin, Utah: A unique model for a basin centered gas accumulation (abs.): AAPG Bulletin, v. 81, no. 7, p. 1229.

Martini, A. M., L. M. Walter, J. M. Budai, T. C. W. Ku, C. Kaiser, and M. Schoell, 1998, Genetic and temporal relations between formation waters and biogenic methane: Upper Devonian Antrim Shale, Michigan Basin, U.S.A.: Geochimica et Cosmochimica Acta, v. 62, p. 1699–1720, doi:10.1016/S0016-7037(98)00090-8.

Martini, A. M., L. M. Walter, J. M. Budai, T. C. W. Ku, J. C. McIntosh, and M. Schoell, 2003, Microbial production and modification of gases in sedimentary basins: A geochemical case study from a Devonian Shale gas play, Michigan Basin: AAPG Bulletin, v. 87, p. 1355–1375, doi:10.1306/031903200184.

McAuliffe, C. D., 1978, Chemical and physical constraints on petroleum migration with emphasis on hydrocarbon solubilities in water: AAPG Short Course, Physical and Chemical Constraints on Petroleum Migration, April 9, Oklahoma City, Oklahoma, 213 p.

McIntosh, J. C., and L. M. Walter, 2005, Volumetrically significant recharge of Pleistocene glacial meltwaters into epicratonic basins: Constraints imposed by solute mass balances: Chemical Geology, v. 222, p. 292–309, doi:10.1016/j.chemgeo.2005.07.010.

McIntosh, J. C., L. M. Walter, and A. M. Martini, 2004a, Extensive microbial modification of formation water geochemistry: Case study from a midcontinent sedimentary basin, United States: Geological Society of America Bulletin, v. 116, no. 5/6, p. 743–759, doi:10.1130/B25371.1.

McIntosh, J. C., L. M. Walter, and A. M. Martini, 2004b, Geochemical modification of Late Devonian shale formation waters via microbial methanogenesis: Geological Society of America Bulletin, v. 116, p. 220–237.

McPherson, B. J. O. L., and J. D. Bredehoeft, 2001, Over-pressure in the Uinta Basin, Utah: Analysis using a three-dimensional basin evolution model: Water Resources Research, v. 37, no. 4, p. 857–871, doi:10.1029/2000WR900260.

Monson, B., and J. Parnell, 1992, The origin of gilsonite vein deposits in the Uinta Basin, *in* T. D. Fouch, V. F. Nuccio, and T. C. Chidsey, eds., Hydrocarbon and mineral resources of the Uinta Basin, Utah and Colorado: Salt Lake City, Utah, Utah Geological Association, p. 257–270.

Naftz, D. L., 1996, Geochemistry of selected aquifers in Tertiary rocks of the upper Colorado River Basin in Wyoming, Colorado, and Utah: U.S. Geological Survey Water-Resources Investigations Report 95-4065, 45 p.

Nuccio, V. F., and T. D. Fouch, 1992, Thermal maturity of the Mesaverde Group, Uinta Basin, Utah, *in* The petroleum system—Status of research and methods: Denver, Colorado, U.S. Geological Survey, p. 70–77.

Nuccio, V. F., and L. N. R. Roberts, 2005, Thermal maturity and oil and gas generation history of petroleum systems in the Uinta-Piceance Province, Utah and Colorado, *in* Petroleum systems and geologic assessment of oil and gas in the Uinta-Piceance Province, Utah and Colorado: U.S. Geological Survey Digital Data Series DDS-69-B, 35 p.

Nuccio, V. F., J. W. Schmoker, and T. D. Fouch, 1992, Thermal maturity, porosity, and lithofacies relationships applied to gas generation and production in Cretaceous and Tertiary low-permeability (tight) sandstones, Uinta Basin, Utah, *in* T. D. Fouch, V. F. Nuccio, and T. C. Chidsey Jr., eds., Hydrocarbon and mineral resources of the Uinta Basin, Utah and Colorado: Utah Geological Survey, Utah Geological Association Guidebook, no. 20, p. 77–94.

Osmond, J. C., 1990, Greater Natural Buttes field, Uinta Basin, Utah: An example of enhanced tight sands gas accumulation (abs.): AAPG Bulletin, v. 74, no. 5, p. 735.

Parkhurst, D. L., L. N. Plummer, and D. C. Thorstenson, 1982, Balance—A computer program for calculating mass transfer for geochemical reactions in ground water: U.S. Geological Survey Water Resources Investigations Report 82–14, 29 p.

Picard, M. D., ed., 1985, Geology and energy resources, Uinta Basin of Utah: Utah Geological Survey, Utah Geological Association Guidebook 12, 350 p.

Pitman, J. K., T. D. Fouch, and M. B. Goldhaber, 1982, Depositional setting and diagenetic evolution of some Tertiary unconventional reservoir rocks, Uinta Basin, Utah: AAPG Bulletin, v. 66, p. 1581–1596.

Pitman, J. K., K. J. Franczyk, and D. E. Anders, 1988, Diagenesis and burial history of nonmarine Upper Cretaceous rocks in the central Uinta Basin, Utah: U.S. Geological Survey Bulletin, v. 1787-D, 24 p.

Price, L. C., and M. Schoell, 1995, Constraints on the origins of hydrocarbon gas from com positions of gases at their site of origin: Nature, v. 378, p. 368–371, doi:10.1038/378368a0.

Rice, C. A., 2003, Production waters associated with the Ferron coalbed methane fields, central Utah: Chemical and isotopic composition and volumes: Goal Geology, v. 56, p. 141–169.

Rice, D. D., 1983, Relation of natural gas composition to thermal maturity and source rock type in San Juan Basin, northwestern New Mexico and southwestern Colorado: AAPG Bulletin, v. 67, p. 1199–1218.

Rice, D. D., T. D. Fouch, and R. C. Johnson, 1992, Influence of source rock type, thermal maturity, and migration on composition and distribution of natural gases, Uinta Basin, Utah, *in* T. D. Fouch, V. F. Nuccio, and T. C. Chidsey Jr., eds., Hydrocarbon and mineral resources of the Uinta Basin, Utah and Colorado: Utah Geological Association Guidebook 20, p. 95–110.

Robson, S. G., and E. R. Banta, 1995, Ground water atlas of the United States, segment 2 Arizona, Colorado, New Mexico, and Utah: U.S. Geological Survey Investigations Atlas 730-C, 32 p.

Ruble, T. E., M. D. Lewan, and R. P. Philp, 2001, New insights on the Green River petroleum system in the Uinta Basin from hydrous pyrolysis experiments: AAPG Bulletin, v. 85, no. 8, p. 1333–1371.

Schamel, S., 2005, Shale gas reservoirs of Utah: Survey of an unexploited potential energy resource: Utah Geological Survey Open-File Report 461, 114 p.

Schmoker, J. W., 2002, Resource-assessment perspectives for unconventional gas systems: AAPG Bulletin, v. 86, no. 11, p. 1993–1999.

Schmoker, J. W., T. D. Fouch, and R. R. Charpentier, 1996, Gas in the Uinta Basin, Utah: Resources in continuous accumulations: The Mountain Geologist, v. 33, no. 4, p. 95–104.

Schoell, M., 1980, The hydrogen and carbon isotopic composition of methane from natural gases of various origins: Geochimica et Cosmochimica Acta, v. 44, p. 649–661, doi:10.1016/0016-7037(80)90155-6.

Schoell, M., 1983, Genetic characterization of natural gases: AAPG Bulletin, v. 67, p. 2225–2238.

Scott, A. R., W. R. Kaiser, and W. B. Ayers Jr., 1994, Thermogenic and secondary biogenic gases, San Juan Basin, Colorado and New Mexico—Implications for coalbed gas producibility: AAPG Bulletin, v. 78, no. 8, p. 1186–1209.

Shurr, G. W., and J. L. Ridgley, 2002, Unconventional shallow biogenic gas systems: AAPG Bulletin, v. 86, no. 11, p. 1939–1969.

Spencer, C. W., 1987, Hydrocarbon generation as a mechanism for overpressuring in Rocky Mountain region: AAPG Bulletin, v. 71, no. 4, p. 368–388.

Stueber, A. M., and L. M. Walter, 1994, Evidence for glacial recharge and paleohydrologic flow systems in the Illinois Basin: Origins of salinity and mixing relations in Ordovician Carbonate (Galena) Formation waters: Geological Society of America Bulletin, v. 106, p. 1430–1439, doi:10.1130/0016-7606(1994)106<1430:GRAPFS>2.3.CO;2.

Surdam, R. C., and K. O. Stanley, 1980, Effects of changes in drainage-basin boundaries on sedimentation in Eocene Lakes Gosiute and Uinta of Wyoming, Utah, and Colorado: Geology, v. 8, p. 135–139, doi:10.1130/0091-7613(1980)8<135:EOCIDB>2.0.CO;2.

Szpakiewicz, M., and A. G. Collins, 1985, Hydrochemical study of the Upper Cretaceous and Lower Tertiary formations

in the Uinta, Piceance and Green River basins: Implications for oil- and gas-related problems: Topical Report for U.S. Department of Energy, DE-FC22-83FE60149, 70 p.

Tabet, D. E., and J. C. Quick, 2001, Potential Neslen Formation fairway for coalbed gas in the eastern Uinta Basin, Utah (abs.): AAPG Annual Convention Program, v. 10, p. A197.

Topographic Map Series, NJ 12-3 (Grand Junction), 1962, Amy Mapping Service, Western United States, scale 1:250,000, 1 sheet.

USGS (U.S. Geological Survey), 2002, Petroleum systems and geologic assessment of oil and gas in the Uinta-Piceance Province, Utah and Colorado: USGS Digital Data Series 069-B, http://pubs.usgs.gov/dds/dds-069/dds-069-b /chapters.html (accessed July 20, 2007).

USGS, 2009, U.S. Geological Survey water data for the nation: U.S. Geological Survey National Water Information System, Web Interface: http://waterdata.usgs.gov/nwis (accessed October 10, 2005).

USWP (Utah State Water Plan), 1999, Utah State Water Plan —Uinta Basin, Utah Board of Water Resources, prepared by the Division of Water Resources of the State Water Plan Steering Committee: http://www.water.utah.gov /planning/swp/unitah/ (accessed August 10, 2007).

Walter, L. M., A. M. Stueber, and T. J. Huston, 1990, Br-Cl-Na systematics in Illinois Basin fluids: Constraints on fluid origin and evolution: Geology, v. 18, p. 315–318, doi:10 .1130/0091-7613(1990)018<0315:BCNSII>2.3.CO;2.

Walter, L. M., J. M. Budai, A. Martini, and T. C. W. Ku, 1997, Hydrogeochemistry of the Antrim Shale in the Michigan Basin: Final Report of the Gas Research Institute, 5093-220-2704, 98 p.

Wanty, R. B., J. K. Pitman, and T. D. Fouch, 1991, Ground-water chemistry and diagenetic reactions in Tertiary sandstone of the Green River and Wasatch formations, Uinta Basin, Utah, in Evolution of sedimentary basins— Uinta and Piceance basins: U.S. Geological Survey Bulletin, no. 1787, 21 p.

Willett, S. D., and D. S. Chapman, 1987, On the use of thermal data to resolve and delineate hydrologic flow systems in sedimentary basins: An example from the Uinta Basin, Utah, in Proceedings of the Third Annual Canadian/American Conference on Hydrogeology: Dublin, Ohio, National Water Well Association, p. 159–168.

Willett, S. D., and D. S. Chapman, 1989, Temperatures, fluid flow and heat transfer mechanisms in the Uinta Basin (abs.), in A. E. Beck and G. Garven, eds., Hydrologic regimes and their subsurface thermal effects: Proceedings of the 1987 International Union of Geodesy and Geophysics: Washington, D.C., American Geophysical Union, p. 29–33.

Zhang, Y., M. Person, E. Merino, and M. Szpakiewcz, 2005, Evaluation of soluble benzene migration in the Uinta Basin: Geofluids, v. 5, no. 2, p. 106–123, doi:10.1111/j .1468-8123.2005.00102.x.